For Reference

NOT TO BE TAKEN FROM THIS ROOM

For Reference

NOT TO BE TAKEN FROM THIS ROOM

Ex Libris
Universitatis
Albertaensis

UNIVERSITY OF ALBERTA
QUAECUMQUE VERA

University of Alberta
Printing Department

Digitized by the Internet Archive
in 2018 with funding from
University of Alberta Libraries

https://archive.org/details/Rankin1960

Thesis
1960 (F)
#1D

THE UNIVERSITY OF ALBERTA

# A THEORETICAL AND EXPERIMENTAL STUDY OF STRUCTURES IN THE MAGNETO-TELLURIC FIELD

A THESIS

SUBMITTED TO THE FACULTY OF GRADUATE STUDIES

IN PARTIAL FULFILMENT OF THE REQUIREMENTS FOR THE DEGREE

OF DOCTOR OF PHILOSOPHY

DEPARTMENT OF PHYSICS

by

D. Rankin

Windsor, Ontario

September, 1960

# ACKNOWLEDGEMENTS

It is fitting that I preface this work with the thanks due to those people who helped make it possible, and I make special mention here of the following:

Professor G. D. Garland, who, in the course of many interesting discussions, stimulated my interest in this problem, and whose advice and counsel forwarded the progress of this research.

Professor K. Vozoff, who gave unstintingly of his time and experience at every critical period in this work.

Professor L. H. Trainor, whose interest in my progress and specific assistance in certain theoretical aspects of this thesis are deeply appreciated.

Among the many other members of the Physics Department of the University of Alberta, I would like to thank Mr. Walter Corfield, Mr. William Murray, and Mr. Robert Ellis.

I am indebted for financial support, to the grant by the National Research Council to the Geophysics Group of the University of Alberta.

Finally, I wish to thank my wife, Sophie, who typed and helped edit this thesis as a small final contribution to her major assistance, without which this work could neither have been started nor completed.

# A THEORETICAL AND EXPERIMENTAL STUDY OF STRUCTURES IN THE MAGNETO-TELLURIC FIELD

## ABSTRACT

The general problem of interpreting magneto-telluric field measurements is a difficult one, chiefly because exact solutions seem possible only for the simplest geological geometries. Because of this, an attempt was made to construct a realistic model of the earth-ionospheric current system. Measurements were made on horizontal layer and fault models for the case of magnetic polarization. These were compared with the exact solutions of Cagniard and of d'Erceville and Kunetz in order to evaluate the model system. Agreement was found to be reasonable, considering the complexity of conditions in the laboratory.

The boundary-value problem of the dike in a two layer earth was then solved, again for the case of magnetic polarization. Model measurements were extended to include dikes and these results when compared with those computed from the exact solution, were in reasonable agreement with one another.

TABLE OF CONTENTS


Page

Chapter I: Introduction, Summary, and Historical Review ..... 1

System of Units ..... 2

Historical ..... 3

Chapter II: Description of Magneto-Telluric Fields

General Properties ..... 11

Special Properties Applicable to a Model Study ..... 21

Chapter III: General Method of Solution and Interpretation for a Multi-Layered Earth

Plane Waves Incident on a Multi-Layered Earth ..... 25

Single Layered Earth ..... 27

Double Layered Earth ..... 27

Law of Similitude ..... 29

Presentation of Data ..... 31

Interpretation in Case of Three Formations ..... 34

Chapter IV: Extension of Theory for Dikes in Two Layered Earth..... 37

Case I - Infinitely Resistive Substratum ..... 39

Case II - Infinitely Conductive Substratum ..... 45

Presentation of Data and Interpretation for Faults and Dikes.... 47

Continued Page

Chapter V: The Real Earth and the Laboratory Model ..... 52

Chapter VI: Apparatus and Procedure ..... 57

Chapter VII: Results, Interpretation, and Conclusions

Frequency Analysis of the Layered Earth ..... 66

Discussion of Theoretical Results for the Dike ..... 70

Experimental Results ..... 79

Chapter VIII: Conclusions and Suggestions for Further Work ..... 85

Appendix I: A Homogeneous Conducting Half Space .. 87

Appendix II: Two Layered Earth ..... 89

Appendix III: Special Cases of a Two Layered Earth

Infinitely Resistive Substratum...92

Infinitely Conducting Substratum..95

Appendix IV: Fault in a Two Layered Earth

Infinitely Resistive Substratum...97

Infinitely Conducting Substratum.100

Bibliography ..... 102

Continued Page

Table 1: Depths of penetration of magneto-telluric field..... 16

Table 2: Amplitude of magnetic field ..... 16

Table 3: Resistivity of various earth constituents.. 52

Table 4: Extrapolation of model to geological dimensions ..... 67

Table 5: Parameters of computed curves ..... 71

Figure 1: Geometrical arrangement for a layered earth ..... 18

Figure 2: Magneto-telluric field components at a fault ..... 21

Figure 3: Distortion of a field due to a thin conducting layer ..... 24

Figure 4: Geometrical arrangement for an n-layered earth ..... 25

Figure 5: Master curves of apparent resistivity for a two layered earth ..... 35

Figure 6: Master curves of phase angle for two layered earth ..... 36

Figure 7: Computed curves for a three layer case ... 36

Figure 8: A fault in a two layered earth ..... 37

Figure 9: A dike in a two layered earth ..... 38

Figure 10: Schematic diagram of experimental arrangement ..... 58

Figure 11: Frequency analysis of model results ..... 69

Figure 12: Computed and experimental values of magneto-telluric ratio for a fault at high frequency ..... 72

Figure 13: Computed and experimental values of magneto-telluric ratio for a fault at low frequency ..... 73

continued Page

Figure 14: Computed and experimental values of magneto-telluric ratio for a conducting dike at high frequency ..... 74

Figure 15: Computed and experimental values of magneto-telluric ratio for a conducting dike at low frequency ..... 75

Figure 16: Computed and experimental values of magneto-telluric ratio for a resistive dike at high frequency ..... 76

Figure 17: Computed and experimental values of magneto-telluric ratio for a resistive dike at low frequency ..... 77

Figure 18: Magneto-telluric ratio over high contrast dike with deep overburden ..... 81

Figure 19: Magneto-telluric ratio over high contrast dike with shallow overburden... 83

Figure 20: Variation in magnetic field over discontinuities..... 84

Figure A: Earth Current System, after Gish ..... 6

Figure B: Instrument section; audio-oscillator, power amplifier, and frequency counter... 59

Figure C: Wooden tank, containing layer of solution and graphite dike ..... 59

Figure D: Photograph of signals on oscilloscope screen ..... 60

# CHAPTER I

## INTRODUCTION, SUMMARY, AND HISTORICAL REVIEW

The ever increasing interest in electro-magnetic interactions with the earth can be attested to by the number of laboratories pursuing research in this field and the number of meetings devoting time to considerations of the subject. The subject is of interest not only from the more basic scientific point of view but also from practical considerations in radio and general signal propagation, and in economic exploration methods.

Since a major interest of the geophysics group at the University of Alberta is in the field measurements of the magneto-telluric effect, it was felt that model studies of the phenomenon would be of considerable importance in developing an understanding of the subject. Despite the general importance of such studies, no true electro-magnetic model of a layered earth has, to date, been described in the literature.

The difficulties involved in an electro-magnetic model study will become apparent in the body of this thesis. The difficulties involved in field measurements are already well known and well described in the literature, and will be touched on at a later point in this work.

System of Units

In all the theoretical developments to follow em cgs units will be employed. In all the practical applications and discussion of them, the so-called "practical" units will be employed. There is no loss of generality in this procedure nor are there any particular complications; this procedure merely follows that of the important writers on the subject who are presently available in English translation and will enable the interested reader of this work to read the references with no further transformation of units. The "practical" units are those employed by the exploration geophysicist and are related to the em units as follows:

| | |
|---|---|
| H measured in gammas | 1 em unit = $10^5$ $\gamma$ |
| E measured in mv/km | 1 em unit = 1 mv/km |
| lengths measured in km | 1 em unit = $10^{-5}$ km |
| $\rho$ measured in ohm-meters | 1 em unit = $10^{-11}$ ohm-meters. |

Thus, for example, skin depth which in the rationalized mks system is $\sqrt{\frac{\rho T}{\pi \mu_0}}$ becomes in the em cgs units

$$d = \frac{1}{2\pi}\sqrt{\rho T}$$

where T is the period, and in the "practical" units:

$$d = \frac{1}{2\pi}\sqrt{10\,\rho T}.$$

Other important quantities have similarly simple transformations which will appear at the appropriate places

in this work.

We will consider only non-magnetic media where $\mu = 1$ and $\varepsilon = \varepsilon_o$.

Historical

All geophysical investigations of the subsurface nature of the earth's crust must of necessity depend on contrasts in the physical parameters of the various sub-surface regions. One of the most pronounced of such contrasts can be observed in magnetometer readings over regions where magnetic materials lie included in non-magnetic country rock. Similarly since the resistivity of the earth could be expected to vary greatly from point to point, one might expect to observe pronounced contrasts when electrical or electro-magnetic measurements are carried out. An example is the case of a saturated salt solution with a resistivity of the order of approximately $10^{-2}$ ohm-meters and dry salt with a resistivity of the order of 100 ohm-meters, lying adjacent to each other at the edge of salt plugs. Another example where pronounced discontinuities in resistivities occur is the case of massive sulphides in an unmineralized environment. Indeed when the early applications of electric and electro-magnetic methods were made they appeared to offer tremendous possibilities for successful exploration, and they were and are successful within the limits which still prescribe them.

In the earlier methods of exploration a source is set up, either D.C., in which case the depth of penetration depends on the distance between electrodes implanted in the surface of the earth; or A.C., in which case either a magnetic dipole or a long line is used and the depth of penetration depends both on the skin effect and the appropriate inverse geometric factor. Whenever such sources are used the practical limits of exploration are restricted to a few hundred feet, whereas in general the answers required in geophysics have no such modest requirements.

Naturally occuring telluric or ground currents were first postulated by Davy in 1821. Though Faraday in 1831 was convinced of their existence as a result of his work on electro-magnetic induction, the primitive equipment available at the time did not permit their detection. Barlow (1849), as a result of studies of the disturbances created in the English telegraph lines, was the first to obtain convincing evidence that such currents do flow in the earth, these disturbances being most pronounced during periods of magnetic activity. Toward the end of the 19th century many magnetic observatories included studies of telluric currents as part of their programs. The number of stations doing so has varied, but records continuous over many years do exist. The major preoccupation of those concerned with these earlier studies of telluric currents was the origin and nature of these currents.

While the correlation of telluric current and magnetic field was appreciated, the difficulties of analysis and instrumentation and the seeming lack of positive results caused a fluctuation in interest in the subject and consequently in the number of stations making the dual observations. The diurnal variations were analyzed by Gish (1939) on the basis of only twelve world wide stations, and on the basis of his analysis he constructed a pattern of current distribution as shown in Figure A. The increased activity, especially since the inception of the I.G.Y., has resulted in a large increase in the number of permanent stations, forty as of 1957, with another twenty projected for immediate implementation.

The wealth of frequency components available makes possible the study of a wide range of specific problems, ranging from frequencies suitable for groundwater, solid, and liquid mineral exploration, to geophysical studies of current distribution in the lower mantle and core. Areas such as Japan (Rikitake(1952, 1953, 1955)), and Germany (Bartels (1954)) display anomalously high magnetic variations with periods of approximately twenty minutes. This indicates anomalously large current distributions at depths of some hundreds of km with currents of the order of 5,000 amperes.

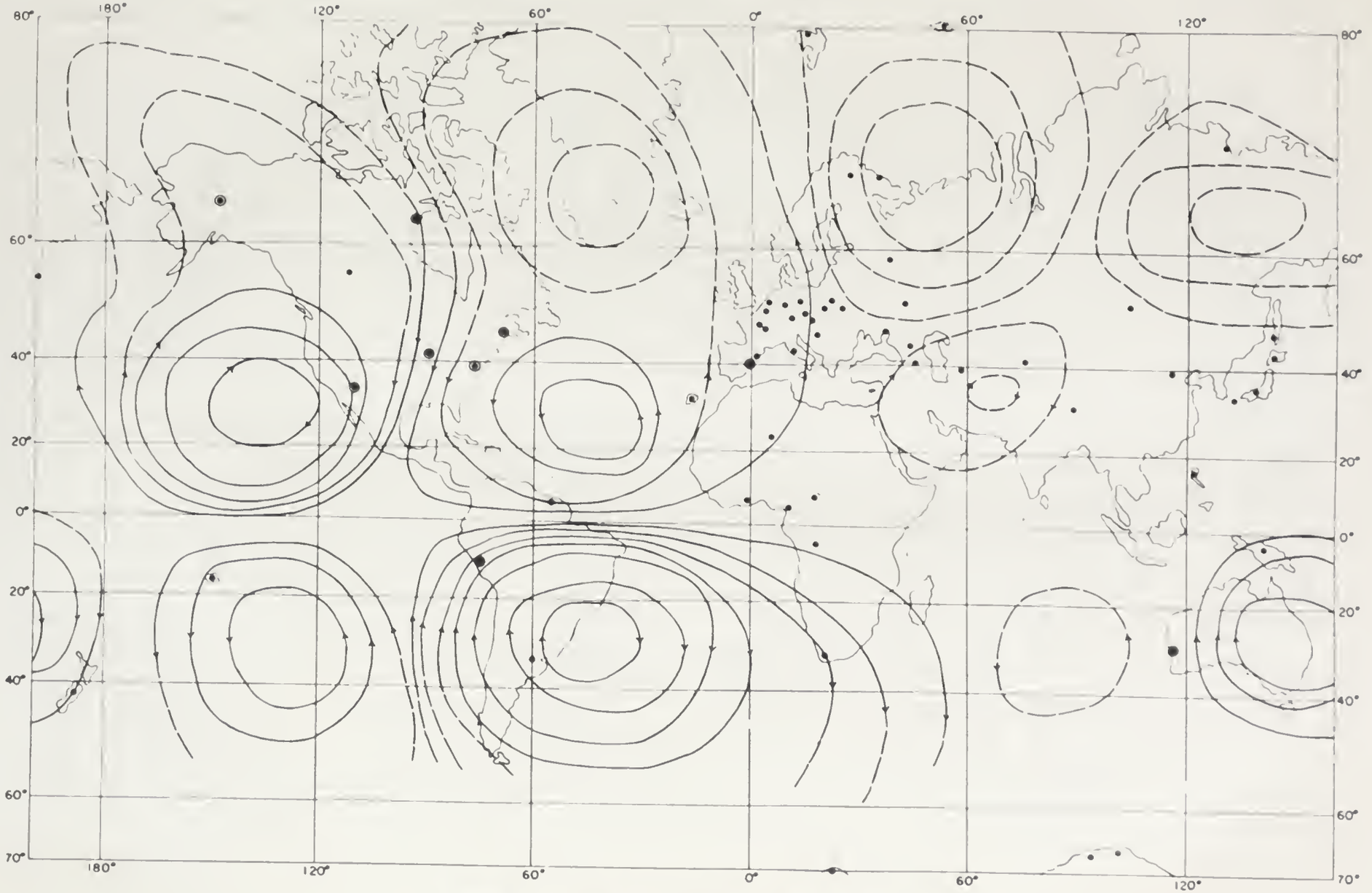


EARTH CURRENT SYSTEM – 18h. G.M.T.
(AFTER GISH, 1936)

● Stations used by Gish

FIGURE A

• Stations in operation or projected, 1957

One can distinguish between the telluric method, which was highly developed in France and Eastern Europe as an exploration method shortly before World War II, and the magneto-telluric method, the name coined by Cagniard (1953). The possibility of the use of the telluric method for exploration was first suggested by Schlumberger in 1921. In this method a base station is used in conjunction with a movable field station. It obviously requires that the telluric currents are uniform at least up to the boundary of the region being explored. We will discuss this question in detail in the next section. This uniformity is all that is required, no further knowledge regarding the nature of the phenomenon being necessary.

Some of the workers in this method considered the associated magnetic variations as being the Biot and Savart field due to flow of current, in which case $\vec{E}$ and $\vec{H}$ should be in phase, others considered a rather simple case of induction in which case $\vec{E}$ and $\vec{H}$ should be $90^{\circ}$ out of phase. The scarcity of data on the simultaneous measurement and lack of knowledge of the electrical properties of the earth did not assist a clarification of the ideas regarding the phenomenon. However, as in many geophysical methods, a lack of understanding of the basic theory does not preclude the possibility of some success in its application; all that is really necessary is uniformity of the source and a contrast that can be

measured.

The magneto-telluric method consists of a simultaneous measurement of the electric and magnetic field components of an electro-magnetic wave; the magnetic field measured at the surface of the earth and the electric field measured as a potential gradient in the surface of the earth. The method may be alternatively called a "generalized impedance method" since in the analysis the electric field and magnetic field appear as a ratio $\frac{E}{H}$. This concept of impedance is due to Schelkunoff (1938). The magneto-telluric method, besides having definite advantages in principle, especially in that phase angle offers a second diagnostic criterion, also has a practical advantage over the telluric method in that no base station is required, and, further, the uniformity of the field is required to a much more restricted degree. The basic ideas of the magneto-telluric method are a recent development and were motivated according to Cagniard (1956) by the lack of correlation between the predictions of the spherical harmonic analysis of Schuster (1889) and Chapman (1919) and the field measurements at observatories, as well as inconsistencies of the telluric method. In 1950 Tikhonov suggested the method as a tool for exploration at great depths while almost simultaneously Kato and Kikuchi (1950) showed that some

measurements they made on phase angles between the magnetic and telluric fields could be explained on the basis of a two-layered earth. A series of papers by Rikitake (1952), Tikhonov and Lipskaia (1952), and Lipskaia (1953) were devoted to various aspects of this phenomena. Cagniard (1953) published a very comprehensive paper on the magneto-telluric method in which he developed graphical methods of considerable usefulness for interpretative purposes. As Cagniard envisioned it, the magneto-telluric method was suited to the large scale exploration of sedimentary basins.

It is one of the facts of nature that the earth's crust is more distinguished by irregularities than by regularities, and while layered sedimentary basins do exist, of equal interest are those very irregularities which give promise of providing economically valuable mineral resources or valuable clues to the geological development of the earth's crust.

Neves (Ph.D. Thesis 1957) and d'Erceville and Kunetz (1959) have attacked the problem of a vertical discontinuity, i.e. a fault, in a layered earth for certain special cases. The method of the latter will be discussed in detail in Appendix IV.

The theoretical problem of a fault belongs to a famous class known as the "problems of the finitely conducting wedge". In the more general case these

problems have not only remained unsolved, but have not even as yet been explicitly formulated. In certain special cases, which fortunately are geophysically significant, approximate solutions can be obtained. It is one of the purposes of this work to investigate the adequacy of these solutions. Another purpose is to extend the theory to certain cases of a dike, and also to study these cases experimentally. The theoretical development of the latter cases appears in Chapter IV.

# CHAPTER II

## DESCRIPTION OF THE MAGNETO-TELLURIC FIELDS

### General Properties

Despite the very low frequencies and the fact that the resistivity $\rho$ is the only parameter involved, no simpler formulation of the magneto-telluric effect is possible than is contained in Maxwell's equations. However, considerable simplification follows from the experimentally observed fact that the sources of this effect are such that the fields appear to be propagated as plane waves. The sources are believed to be vast sheets of current in the ionosphere.

Wait (1954) has pointed out that if the sources were to be considered as an arbitrary system of dipoles then the fields as measured at the surface of discontinuity in the x,y horizontal plane must be related thus:

$$E_x = \eta H_y + \frac{\eta}{2\gamma^2}\left[\frac{\partial^2 H_y}{\partial y^2} - \frac{\partial^2 H_x}{\partial x^2} + 2\frac{\partial^2 H_x}{\partial x \partial y}\right] + O(\gamma^{-4})$$

$$-E_y = \eta H_x + \frac{\eta}{2\gamma^2}\left[\frac{\partial^2 H_x}{\partial x^2} - \frac{\partial^2 H_y}{\partial y^2} + 2\frac{\partial^2 H_y}{\partial x \partial y}\right] + O(\gamma^{-4})$$

where

$$\gamma = 4\pi j \sigma \mu \omega - \varepsilon \mu \omega^2$$

is the intrinsic propagation constant of the lower medium, and

$$\eta = \frac{j\mu\omega}{\gamma}$$

is the intrinsic impedance of the lower medium, $\sigma$ being its conductivity.

The above formulation takes into account the curvature of the wave front and the resulting phase angles. For $\sigma = .1$ mho and $\omega$ corresponding to a period of 10 sec.

$$\frac{1}{\gamma} = 35 \text{ km}.$$

For this case when $H_x$, $H_y$ do not vary appreciably over a region of 35 km, the terms in $\frac{1}{\gamma^2}$ can be neglected and

$$E_x = \eta H_y$$
$$E_y = -\eta H_x,$$

i.e., E and H are perpendicular to each other. In this case the simplified treatment of Cagniard (1953), to be treated in some detail in Appendix II, is valid. For longer periods, which are of importance in the method, Wait suggests that such uniformity over distances of 35 km is unlikely, since the sources of the magnetic variation are at heights of only 100 km. However, Wait's argument depends on the assumption that the sources for the longer wave lengths are localized, whereas it is

precisely for the longer wave lengths that the fields appear to be uniform, while it is for the much shorter wave lengths that the sources may be more localized. In this latter case the 100 km heights of the sources does not impose such a severe limitation as for the longer wave lengths and sufficient uniformity is still apparent in actual measurements. Cagniard (1954) insists that localized sources exist only in regions of industrial installations.

Schlumberger and Kunetz (1946) and Kunetz (1953, 1954) have confirmed the similarity of the magneto-telluric fields from regions as widespread as Madagascar, France and Venezuela. The correlation of magneto-telluric activity with sun and auroral activity would seem to indicate the global extent of the phenomenon. In general, the a priori assumption of the magneto-telluric method, that of plane wave propagation, would seem to be justified.

The appropriate equation for the propagation of the magnetic field can be written:

$$\nabla^2 \vec{H} = 4\pi\sigma \frac{\partial H}{\partial t} + \varepsilon \frac{\partial^2 \vec{H}}{\partial t^2} \quad .$$

We will hereafter consider that field components of both E and H depend on time as $e^{j\omega t}$ since any arbitrary spectrum of frequencies can be resolved in theory by Fourier analysis and in practice by suitable filtering.

In this case the propagation equation is reduced to:

$$\nabla^2 \vec{H} = \left[4\pi j\sigma\omega - \varepsilon\omega^2\right]\vec{H} \qquad \underline{\text{II}} - 1$$

In air, where $\sigma = 0$, equation II-1 becomes:

$$\nabla^2 \vec{H} = -\varepsilon\omega^2 \vec{H},$$

while in a medium such as the earth where the second term of equation 1, which is the displacement current term, is negligible, the propagation equation reduces to:

$$\nabla^2 \vec{H} = 4\pi j\sigma\omega \vec{H}.$$

Recalling that for both media $\mu = 1$, and $\varepsilon = \varepsilon_0 = \frac{1}{c^2}$ we see that while the velocity of propagation of the wave in air is C, the velocity of propagation in the earth is $v = \sqrt{\frac{\omega}{2\pi\sigma}}$.

For a period of one second the velocity is $\sqrt{\frac{\rho}{2}}$. For resistivities as large as $10^4$ ohm-meters, a quite high value, the velocity in the earth is still only approximately $2 \times 10^5$ m/sec. Thus, by Snell's Law, a plane wave, even if incident at nearly grazing angle, would be propagated into the earth nearly normal to the surface. This is a result of the situation that in a conducting medium such as the earth, displacement current is negligible.

A solution to the propagation equation for the down-going wave in an infinite homogeneous earth can be written in the form:

$$\vec{H} = \vec{H}_o e^{-\sqrt{4\pi j\sigma\omega}\, z}$$
$$= H_o e^{-\sqrt{2\pi\sigma\omega}\, z}\, e^{-j\sqrt{2\pi\sigma\omega}\, z}$$

We define $d = \frac{1}{\sqrt{2\pi\sigma\omega}}$ in the normal way as the skin depth, the depth at which the amplitude of the field diminishes to $\frac{1}{e}$ of its value at the surface. A list of values of the skin depth in km versus periods and resistivities in ohm-meters is shown in Table I.

From Maxwell's equation:

$$(\nabla \times \vec{H})_x = 4\pi\sigma E_x$$

we can write in the case of H polarized in the y direction:

$$\frac{-\partial H_y}{\partial z} = 4\pi\sigma E_x$$
$$E_x = \sqrt{\frac{j\rho}{2T}}\, H_y$$

or:

$$\rho = 2T \left|\frac{E_x}{H_y}\right|^2$$

In Table 2 is shown the amplitude of H in gammas for E=1 mv/km for various values of $\rho$ and $T$. The two tables are included at this point under the general description of the properties of the fields in order to illustrate

TABLE I

DEPTHS OF PENETRATION GIVEN IN KM (After Cagniard)

| ρ \ T → | 1 sec | 3 sec | 10 sec | 30 sec | 1 min | 2 min | 5 min | 10 min | 30 min |
|---|---|---|---|---|---|---|---|---|---|
| 0.2 | 0.225 | 0.390 | 0.712 | 1.23 | 1.74 | 2.47 | 3.90 | 5.51 | 9.54 |
| 1 | 0.503 | 0.872 | 1.59 | 2.76 | 3.90 | 5.51 | 8.72 | 12.3 | 21.4 |
| 5 | 1.13 | 1.95 | 3.56 | 6.16 | 8.72 | 12.3 | 19.5 | 27.6 | 47.7 |
| 10 | 1.59 | 2.76 | 5.03 | 8.72 | 12.3 | 17.4 | 27.6 | 39.0 | 67.5 |
| 50 | 3.56 | 6.16 | 11.3 | 19.5 | 27.6 | 39.0 | 61.6 | 87.2 | 151 |
| 250 | 7.95 | 13.8 | 25.2 | 43.6 | 61.6 | 87.2 | 138 | 195 | 338 |
| 1,000 | 15.9 | 27.6 | 50.3 | 87.2 | 123 | 174 | 276 | 390 | 675 |
| 5,000 | 35.6 | 61.6 | 113 | 195 | 276 | 390 | 616 | 872 | 1510 |

TABLE 2

AMPLITUDES OF THE MAGNETIC FIELD GIVEN IN $\gamma$ WHEN E IS I Mv/KM (After Cagniard)

| ρ \ T → | 1 sec | 3 sec | 10 sec | 30 sec | 1 min | 2 min | 5 min | 10 min | 30 min |
|---|---|---|---|---|---|---|---|---|---|
| 0.2 | 1 | 1.73 | 3.16 | 5.48 | 7.75 | 11.0 | 17.3 | 24.5 | 42.4 |
| 1 | 0.447 | 0.775 | 1.41 | 2.45 | 3.46 | 4.90 | 7.75 | 11.0 | 19.0 |
| 5 | 0.2 | 0.346 | 0.632 | 1.10 | 1.55 | 2.19 | 3.46 | 4.90 | 8.49 |
| 10 | 0.141 | 0.245 | 0.447 | 0.775 | 1.10 | 1.55 | 2.45 | 3.46 | 6 |
| 50 | 0.0632 | 0.110 | 0.2 | 0.346 | 0.490 | 0.693 | 1.10 | 1.55 | 2.68 |
| 250 | 0.0283 | 0.049 | 0.0894 | 0.155 | 0.219 | 0.310 | 0.490 | 0.693 | 1.2 |
| 1,000 | 0.0141 | 0.0245 | 0.0447 | 0.0775 | 0.110 | 0.155 | 0.245 | 0.346 | 0.6 |
| 5,000 | 0.00632 | 0.0110 | 0.0200 | 0.0346 | 0.0490 | 0.0693 | 0.110 | 0.155 | 0.268 |

the possibilities of the magneto-telluric method, both as to the depth of penetration possible and the easily detected variations in the ratio of E and H with both period and resistivity.

The formulas of the preceeding paragraphs are in em units, whereas the associated tables are in the "practical" units, since for most readers these are easier to visualize both dimensionally and in magnitude than are the em units.

In the theoretical development to follow, we consider that the surface of the earth can be considered as a flat, in the dimensions we are considering. The uniformity of the fields and the direction of propagation in the earth ensure the validity of the approximation.

For our study we will adopt a co-ordinate system with z positive downward. Since we will be concerned with plane waves, which propagate normal to the earth's surface within the medium, we are free to choose our direction of propagation in the positive z-direction for all cases. We are further free to orientate our x,y directions on the surface of the earth to suit the direction of polarization of one of the electro-magnetic vectors. In practice E and H will be measured in mutually perpendicular directions.

Let us choose our co-ordinates such that in free space at large distances from the earth $H=H_y$ and the surface of the earth is the x,y-plane at z=0. A second horizontal interface when it is introduced will be at z=h. Vertical discontinuities, when they are introduced, will lie in the y,z plane, i.e. magnetically polarized cases only will be discussed from a theoretical point of view. The surfaces of discontinuity separate regions differing only in their resistivities. Figure 1 shows the general geometrical arrangements. For simple layered systems with no vertical discontinuities we will consider the surfaces to be infinitely extended in all horizontal directions. Any vertical discontinuities will be in the y,z plane and of infinite extent in the y direction. These may be either dikes or faults.

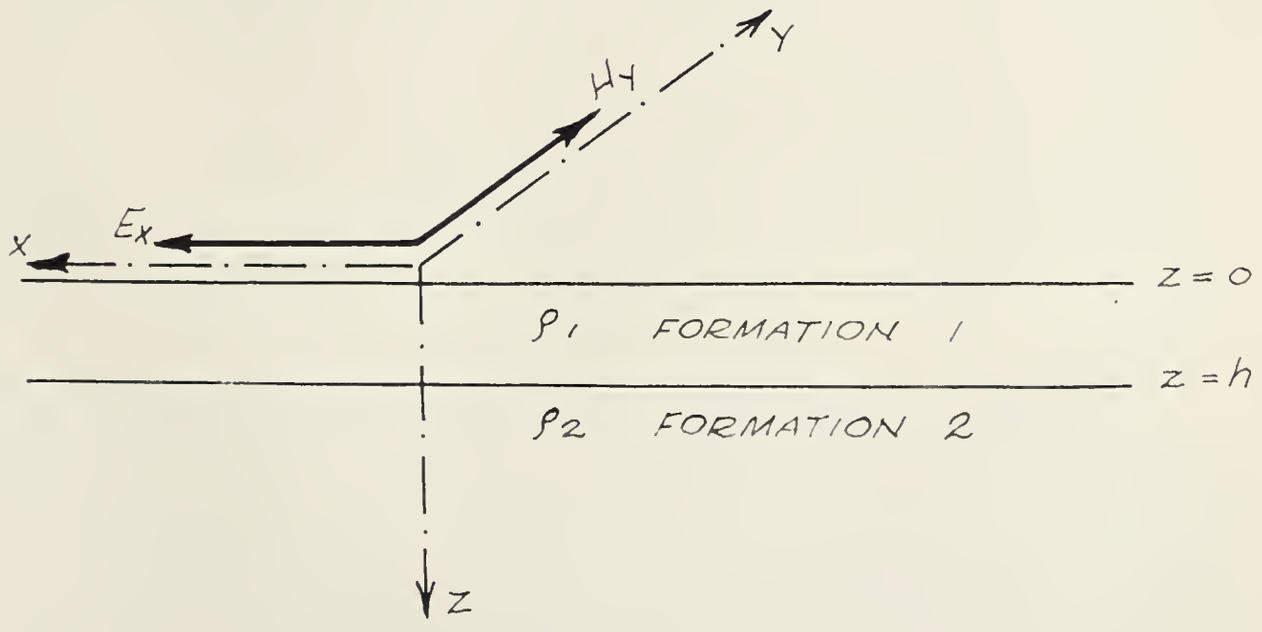


Fig. 1. Geometrical arrangement of a layered earth.

Thus if we write for two of Maxwell's equations:

$$\nabla \times \vec{H} = 4\pi\vec{i} + \frac{\partial \vec{D}}{\partial t} \quad , \qquad \nabla \times \vec{E} = -\frac{\partial \vec{B}}{\partial t}$$

within the media where $\frac{\partial D}{\partial t}$ is negligible in comparison to $4\pi i$ we can re-write:

$$\nabla \times \vec{H} = 4\pi\vec{i} \quad \text{II-2}, \qquad \nabla \times \vec{E} = -j\omega\vec{B}. \quad \text{II-3}$$

From considerations of symmetry we see that:

(1) <u>All partial derivatives with respect to y are identically zero</u>.

(2) <u>$E_y$ is identically zero</u>.

For condition (2) we could as well have written $B_x$ is identically zero.

From the second of Maxwell's equations, as written above, we expand:

$$\frac{\partial E_x}{\partial y} - \frac{\partial E_y}{\partial x} = -j\omega B_z$$

$$\frac{\partial E_z}{\partial y} - \frac{\partial E_y}{\partial z} = -j\omega B_x$$

and observe that $B_x$ and $B_z$ and hence also $H_x$ and $H_z$ are everywhere zero by the two conditions given previously. We originally chose our y axis such that $H=H_y$ for $z >> o$ and now we see that $H \equiv H_y$.

From the first of Maxwell's equations we re-write and expand:

$$\frac{\partial H_z}{\partial y} - \frac{\partial H_y}{\partial z} = +4\pi\sigma E_x$$

$$\frac{\partial H_y}{\partial x} - \frac{\partial H_x}{\partial y} = 4\pi\sigma E_z$$

which gives:

$$E_x = \frac{-\rho}{4\pi} \frac{\partial H_y}{\partial z} \qquad \text{II} - 4$$

$$E_z = \frac{\rho}{4\pi} \frac{\partial H_y}{\partial x} \qquad \text{II} - 5$$

as a result of condition 1 above.

From equation II-3 we can readily deduce that the tangential component of E is continuous across any surface, which gives in our geometry that $E_z$ is continuous across a fault surface.

We observe at this point that the above deductions are valid for the case where one medium is infinitely conducting, $\rho = 0$.

Applying equation II-2, at the upper surface, separating regions where $\rho$ is finite or zero from air where $\rho$ is virtually infinite, we have, $i_z$ being zero, that:

$$\frac{\partial H_y}{\partial x} = 0 ,$$

i.e., at the upper surface $H_y$ is constant even across the trace of the horizontal discontinuity in $\rho$.

If we now solve the propagation equation for $\vec{H}$ for the media we have considered:

$$\nabla^2 \vec{H} = 4\pi\sigma\omega\vec{H}$$

we can then deduce the value of $\vec{E}$ from equations 4 and 5.

Special Properties Applicable to Model Studies

In Figure 2 are illustrated the relationships between the various field components across a fault separating two media in one of which the resistivity is zero. In the medium to the left the incoming wave propagates downward and may be partly reflected at each interface. In the medium to the right where the incoming wave is totally reflected, $E_x$ for the incoming wave just cancels $E_x$ for the reflected wave to give a resulting value $E_x=0$.

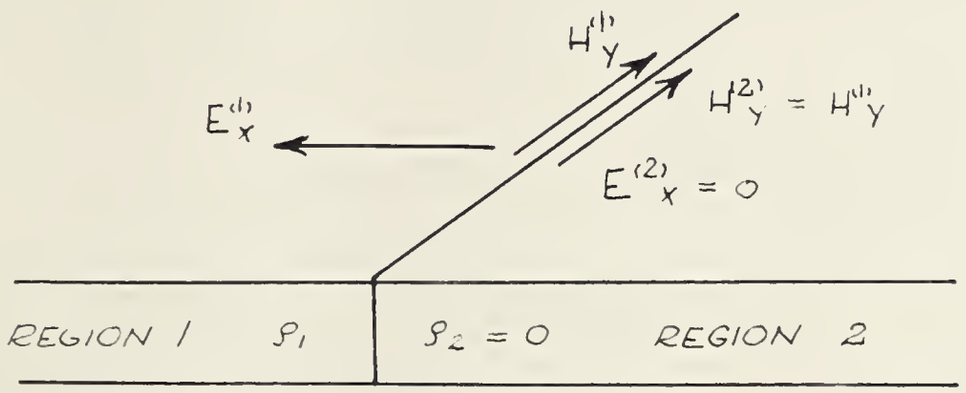


Fig. 2. The magneto-telluric field components at a fault.

The resulting $H_y$ which is continuous across the strike need not be zero on the surface, since $H_y$ for the reflected wave is in the same direction as $H_y$ for the incoming wave. Across the fault $E_z$ is continuous and zero; i.e., there is only an x-component of E and it is non-zero only on the side where $\rho$ is not zero. Charge distributes itself on the interface in such a manner that $E_x$ and $H_y$ are unchanged from the values appropriate to an infinitely extended case in region one and also so that $E_x$ is zero in region two, except possibly for edge effects in the immediate neighbourhood of the upper edge. If at some finite distance to the left we introduce another discontinuity separating a third region of resistivity zero, extending infinitely to the left, the same conditions will hold, therefore in the region in the centre which has finite conductivity the field components are those appropriate to an infinitely-extended layered system. In our model we have attempted to take advantage of these properties and this behaviour of the field components in order to simulate an infinitely extended media within a rather restricted space.

In conducting media of finite resistivity we will assume that in general $H_y$ is a function of x and z; E, since it is derivable from $H_y$, is also a function of x, z. We have already observed that, at distances remote from vertical discontinuities, the dependence on x must

vanish and we have further observed how a perfect conductor causes the field components to be modified. It is only in proximity to structure in media of finite resistivity then, that we expect to find some dependence of $H_y$ on x and therefore a z component of E through the equation:

$$E_z = \frac{\rho}{4\pi} \frac{\partial H_y}{\partial x}.$$

$E_z$ vanishes on the upper surface where $H_y$ is a constant due to the fact that no current flows across this surface. At the vertical interface E must make an abrupt change in direction since $E_z$ is continuous whereas $E_x$ is discontinuous. The magneto-telluric ratios, for this case, measurable along the upper surface where $E_z=0$, is the subject of a paper by d'Erceville and Kunetz which is summarized in Appendix IV.

We recapitulate the qualitative results at this point: at large distances from the fault E is in the x direction, near the fault it has a z component, and in the intervening regions it has intermediate directions.

If we now introduce a thin layer of a perfect conductor on the interface, the direction of E must be changed at least at the surfaces of this conductor in order that there be only an x component of E. The lines of force are distorted from the previous case as

illustrated in Figure 3. If the conducting layer is sufficiently thin in comparison to distances over which individual measurements are made, we will assume that the effect of this infinitely conducting layer can be considered as negligible.

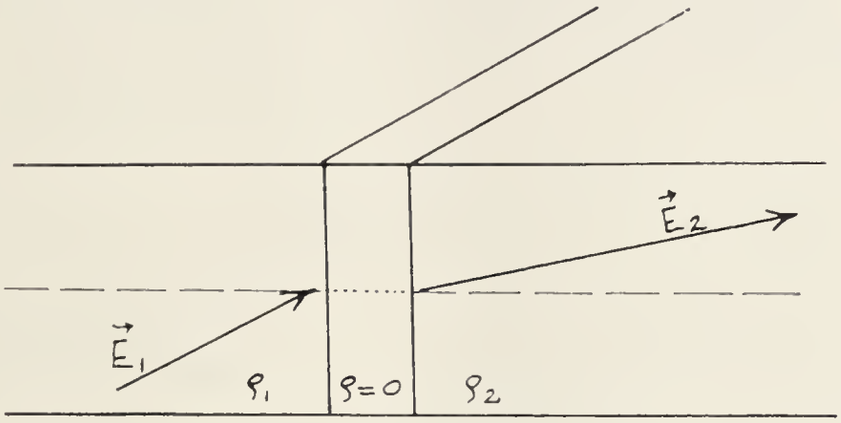


Fig. 3. Distortion of a field due to a thin layer of a perfect conductor.

The application of these latter results to the construction of model faults and dikes will be discussed later in this work.

# CHAPTER III

## GENERAL METHOD OF SOLUTION AND INTERPRETATION FOR MULTI-LAYERED EARTH

### Plane Waves Incident on a Multi-Layered Earth

With the co-ordinate system previously described and illustrated in Figure 4

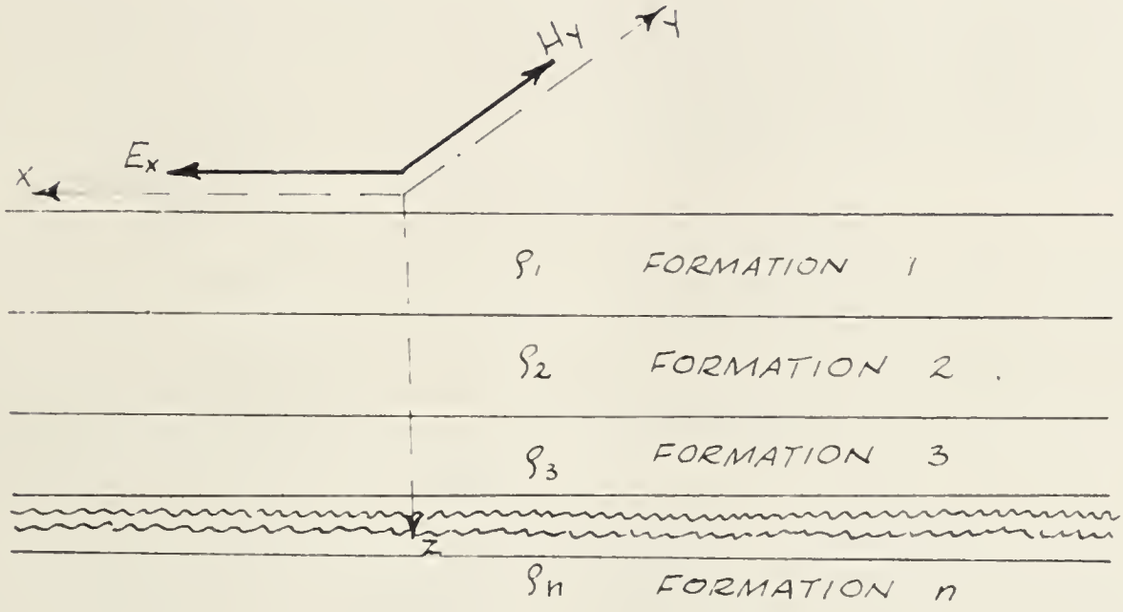


Fig. 4. Geometrical arrangement for an n-layered earth.

we consider a multi-layered conducting earth infinitely extended in the x and y direction, the lowest layer of resistivity $\rho_n$ extending infinitely downward.

The equation for the propagation of H in media where $\mu_i = 1$, $\varepsilon_i = \varepsilon_0$ degenerates into:

$$\nabla^2 \vec{H} = [illegible]$$

as a result of the form of the time dependence and the neglect of displacement current compared to conduction current. For these layers infinitely extended, we can further reduce this equation, by considerations of symmetry, to the ordinary differential equation:

$$\frac{d^2 H_y}{dz^2} = 4\pi j \sigma \omega H_y \,. \qquad \text{III} - 6$$

A solution which satisfies the boundary conditions for any value of x and y and vanishes for $z \to \infty$ can be written down immediately.

$$H_i = A_i e^{\sqrt{j}\frac{z}{\rho_i}} + B_i e^{-\sqrt{j}\frac{z}{\rho_i}} \qquad \text{III} - 7$$

for all layers i = 1, 2, ..... n.

$$\rho_i = \frac{1}{\sqrt{4\pi\sigma\omega}}$$

is $\frac{1}{\sqrt{2}}$ times $d_i$, the skin depth. The terms with $A_i$ represent an upgoing or reflected wave and the terms with $B_i$, a downgoing wave. Hence:

$$H_n = B_n e^{-\sqrt{j}\frac{z}{\rho_n}} \qquad \text{III} - 8$$

since $A_n$ must be zero in the infinitely downward-extending lowest layer.

From the continuity of $H_y$ and $E_x$ at each of n boundaries we can obtain 2n equations from which we can solve for 2n-1 constants $A_i$, $B_i$ in terms of $H_o$, the value

of $H_y$ at the upper boundary. This leaves one equation with which to solve for $E_o$, the value of $E_x$ at the upper boundary. The solutions for certain special cases have been developed by Cagniard. The development is summarized in the Appendices.

Single-Layer Earth Infinitely Extending Downward

We quote the following results from Appendix I:

$$\frac{E_x}{H_y} = \sqrt{\frac{\rho}{2T}}\, e^{j\frac{\pi}{4}}$$

$$\rho = 2T\left|\frac{E}{H}\right|^2$$

and observe that in this simple case the electric field leads the magnetic by $45^o$ and that the resistivity of the layer can be simply derived from the magneto-telluric ratio.

Double-Layered Earth:

(The upper layer of resistivity $\rho_1$, to depth h, the lower layer of resistivity $\rho_2$ infinitely extended downward.)

The results as derived in Appendix 2 give:

$$\frac{E_x}{H_y} = \sqrt{\frac{\rho}{2T}}\ \frac{M}{N}\, e^{j\left(\frac{\pi}{4} + \phi - \psi\right)}$$

where $M, N, \phi$, and $\psi$ defined in the appendix. Recalling from the previous section that for a single homogeneous

layer:

$$\frac{E_x}{H_y} = \sqrt{\frac{\rho}{2T}}\, e^{j\frac{\pi}{4}}$$

we observe that the simplest evidence of a hetereogeneous earth is the departure of the phase angle from $45^{\circ}$.

In order to use the graphical technique so beautifully developed by Cagniard (1953) we follow his procedure and define the apparent resistivity " $\rho_a$ " through the equation:

$$\left|\frac{E}{H}\right| = \sqrt{\frac{\rho_a}{2T}}$$

$$\rho_a = 2T\left|\frac{E}{H}\right|^2 .$$

Then returning to the first equation of this section, we can write:

$$\rho_a = \rho_1 \left(\frac{M}{N}\right)^2 .$$

If one plots $\rho_a$ versus T for each value of $\rho_1$ , then one would obtain a separate family of curves for each value of $\rho_2$ and h.

The phase angle which is also diagnostic of layering is given by:

$$\theta = \frac{\pi}{4} + \phi - \psi .$$

The details can be obtained from the appendices.

Since there is a vast saving in labour to be achieved by a suitable graphical method, we will digress at this point to discuss the law of similitude and return to describe the method of presenting the totality of curves for the two-layer case in one master set, immediately afterward.

The Law of Similitude (Stratton (1941))

Consider two geometrically similar structures with a dimensional ratio:

$$L' = k_\ell L .$$

For our electro-magnetic similitude we will consider:

$$\begin{aligned} \mu' &= \mu = 1 \\ \varepsilon' &= \varepsilon = \varepsilon_0 \\ \rho' &= k_\rho \rho \end{aligned} .$$

The only other variable

$$T' = k_t T .$$

Similitude requires that:

$$\nabla^2 \vec{H}' = 4\pi j \sigma' \omega' \vec{H}'$$

implies

$$\nabla^2 \vec{H} = 4\pi j \sigma \omega \vec{H} .$$

From the former equation

$$\frac{\nabla^2 (k_h \vec{H})}{k_\ell^2} = 4\pi j \frac{\sigma}{k_\rho} \frac{\omega}{k_t} (k_h \vec{H}) ,$$

we obtain the latter, if:

$$K_\ell^2 = K_\rho K_t .$$

Further, from Maxwell's equation:

$$\nabla \times \vec{E} = -\frac{\partial \vec{H}}{\partial t} .$$

We see that dimensionally:

$$\frac{E}{H} = \frac{L}{T} ;$$

then:

$$\frac{E'}{H'} = \frac{K_\ell}{K_t} \frac{E}{H} ,$$

and

$$\frac{\rho_a'}{\rho_a} = \frac{2T'\left(\frac{E'}{H'}\right)^2}{2T\left(\frac{E}{H}\right)^2} = K_t \frac{K_\ell^2}{K_t^2} = K_\rho .$$

Thus the ratio of the apparent resistivities is the same as the ratio of the actual resistivities.

The measurements made on models, as far as size, resistivity and frequency are concerned, have immediate application to a full-size earth. One need only take into account the dimensional ratios

We will proceed now to the presentation of our theoretical curves, as for example, the double-layered earth of the previous section.

Presentation of Data

The values computed from the formula

$$\rho_a = \rho_1 \left(\frac{M}{N}\right)^2$$

can be plotted as the logarithmic ordinates versus $\sqrt{T}$ as the logarithmic abcissa for the various values of the parameters $\rho_1$ , $\rho_2$ and h. If one chooses $\rho_1$ = 1 ohm-meter, h=1 km, then there is only one parameter $\rho_2$ and one obtains a family of curves, one for each value of $\rho_2$ .

The complete set of magneto-telluric curves is now represented by this one family, since we can consider the values of $\rho$ and h as being that of a model, and thus the curves obtained by plotting:

$$\rho_a = 2T \left(\frac{E}{H}\right)^2$$

can be brought into co-incidence with one of the family of theoretical curves by a translation parallel to the ordinates of magnitude $K\rho$ and parallel to the abcissa of magnitude $\sqrt{K_t}$ . Referring once again to Appendix 2, one may write alternatively:

$$\frac{\rho_a}{\rho_1} = 1 + \frac{4 \cos \frac{2h}{d_1}}{m + \frac{1}{m} - 2 \cos \frac{2h}{d_1}} .$$

where:

$$m = \frac{\sqrt{\frac{\rho_2}{\rho_1} + 1}}{\sqrt{\frac{\rho_2}{\rho_1} - 1}} e^{\frac{2h}{d_1}}$$

with $d_1$ the skin depth in the upper medium. The family of curves for $\rho_a$ has an infinite number of points common to each curve. These are given by:

$$\rho_a = \rho_1 \qquad \cos \frac{2h}{d_1} = 0$$

or

$$\frac{2h}{d_1} = \frac{2n+1}{2}\pi$$

for all n.

The point furthest to the right has an abcissa:

$$\frac{2h}{d_1} = \frac{\pi}{2}$$

which gives the result:

$$\rho_a = \rho_1 \quad , \quad \sqrt{T} = 8$$

for the ordinates of the point.

It is customary to plot the phase angle $\theta$ as the ordinate on a linear scale versus $\sqrt{T}$ as abcissa on a logarithmic scle.

We will finally transform to the "practical" units for plotting all the results. In this system

$$\rho_a = .2T\left(\frac{E}{H}\right)^2$$

and the common point of the family of curves is given by:

$$\rho_a = \rho_1 \quad , \sqrt{T} = \frac{8}{\sqrt{10}} .$$

One may further observe that for T sufficiently large, each curve of the family becomes asymptotic to a

finite value except in the case where $\rho_2 = 0$ or $\infty$. This asymptotic value, of course, corresponds to the situation where the upper layer becomes negligible, i. e. the skin depth is very much larger than h. Similarly for high frequencies, the curve approaches the value $\rho_1$, but only by an infinite number of small amplitude oscillations about $\rho_1$.

The amplitude of the shift parallel to the abcissa that must be simultaneously made in this translation process in order to bring the experimental curve into coincidence with the theoretical curve is:

$$x = \sqrt{K_t},$$

but by definition $K_t$ is the ratio of the abcissa of the cross-over point of the theoretical curve as seen on the experimental curve:

$$T' = K_t \left(\frac{s}{\sqrt{10}}\right)^2$$
$$h' = K_\ell h = \sqrt{K_\rho K_t}, \quad h = 1,$$

thus the true thickness of the upper layer

$$h' = \frac{\sqrt{K_\rho 10 T'}}{s}$$

where $K_\rho$ is the translation parallel to the axis of ordinates and $T_1$ is the abcissa of the cross-over point.

$$\rho_1' = K_\rho$$

$\rho_2'$ is the asymptote of the experimental curve for large T as read off the extrapolation of the experimental curves. The interpretation is satisfactory only if the

same translation parallel to the abcissa is required to bring the phase angle curve into coincidence with its theoretical curve. These families of curves are illustrated in Figures 5 and 6.

Interpretation in Case of Three Formations

Under certain favourable conditions the magnetotelluric method is actually much simpler of interpretation than the conventional resistivity method.

Consider a layered system of three formations of resistivity $\rho_1$ , $\rho_2$ and $\rho_3$ , and of thickness $h'$ and $h''$ If $\frac{h''}{h'}$ is sufficiently large then it is possible that the effect of the substratum starts to be appreciable only after the effect of the upper layer has ceased to be effective. In other words, for periods sufficiently long, $\rho_a$ has approached closely to $\rho_2$ and $\theta$ has approached $\frac{\pi}{2}$ before the effect of the third layer has started to make itself felt. The curves of Figure 7 are computed from the theory in Cagniard (1953). We can see that if the curves are cut where indicated, each part can be fitted to one or another of the family for the two-layer case.

Such favourable conditions do not always exist, but a good deal of interpretation can be carried out with a minimum catalogue of computed curves.

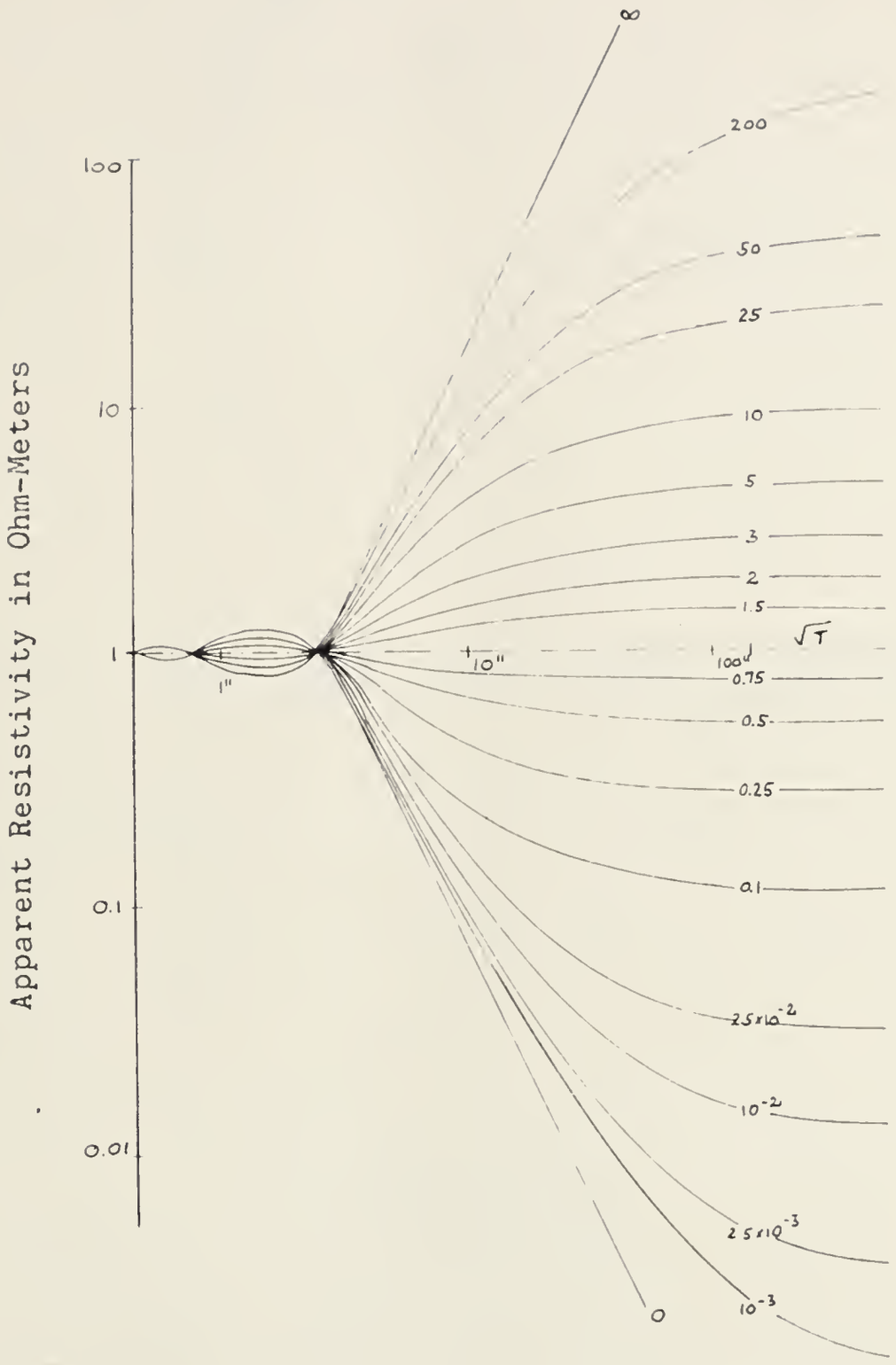


Fig. 5. Master curves of apparent resistivity for magneto-telluric soundings over a two-layer earth.

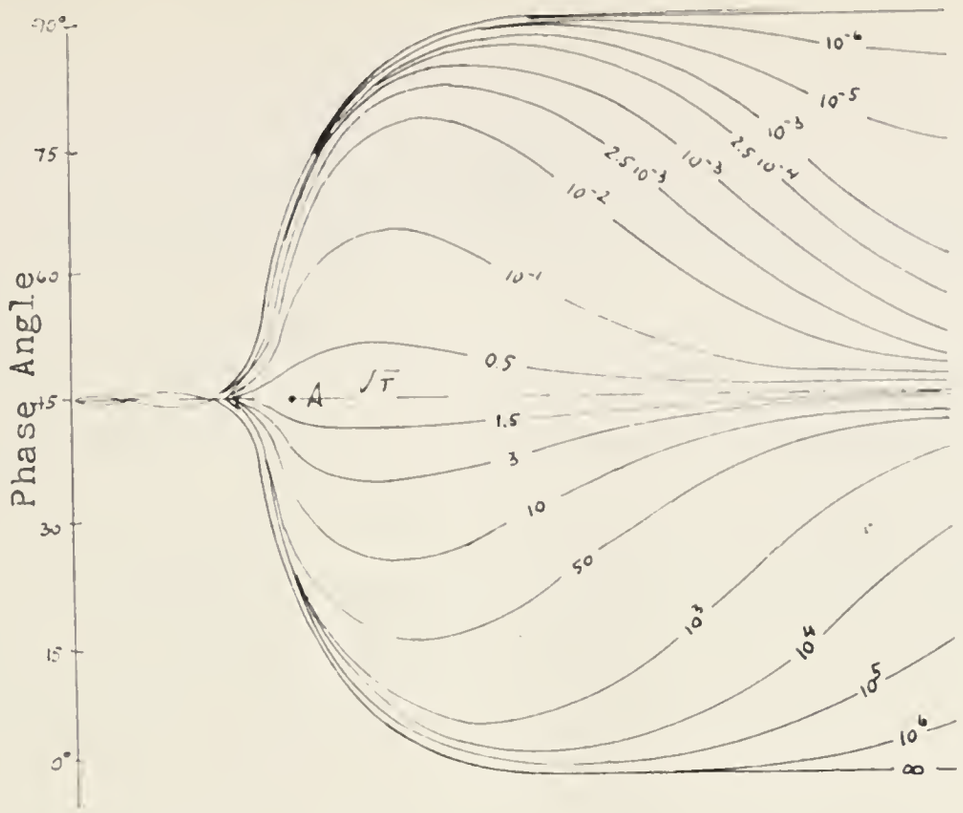


Fig. 6. Master curves of phase angle for magneto-telluric soundings. (after Cagniard, 1953)

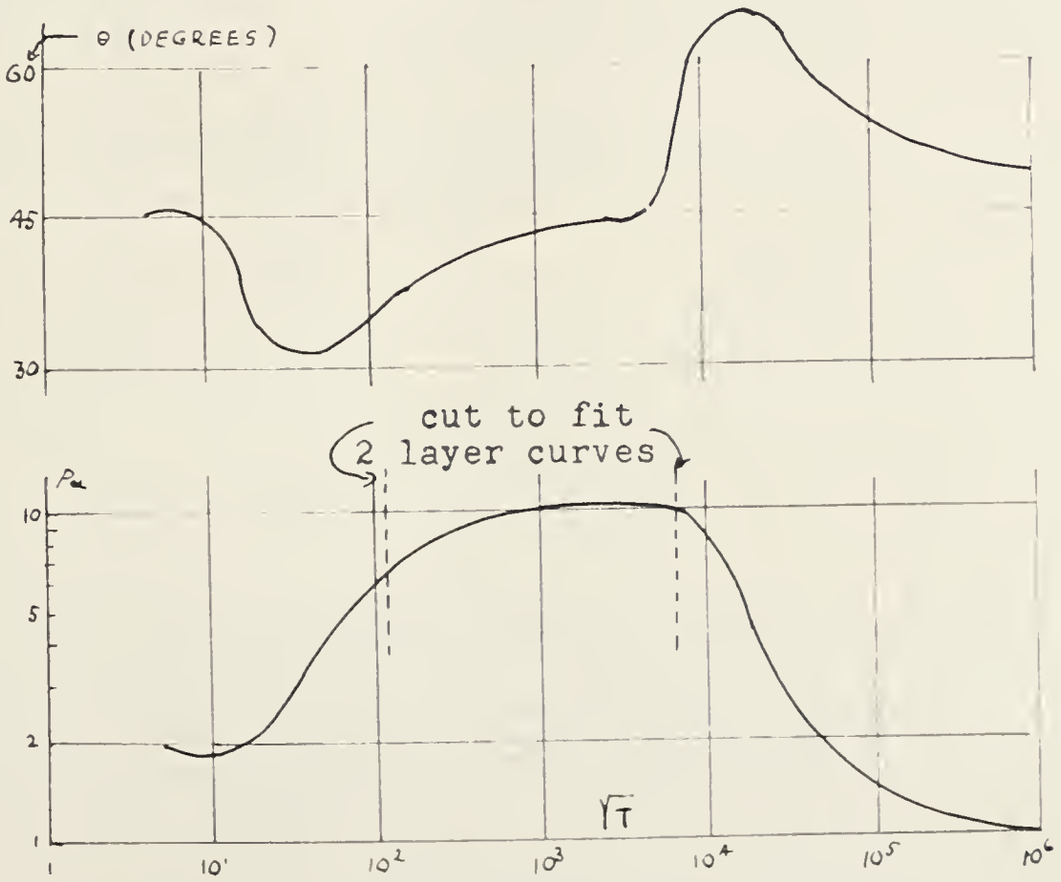


Fig. 7. Computed curves for three-layer case. $h' = 900\ h$, $\rho_1$ , $\rho_2$ and $\rho_3$ in the ratio 2:10:1. (after Cagniard, 1953)

# CHAPTER IV

## EXTENSION TO THE THEORY FOR DIKES IN A LAYERED EARTH

In Appendix IV are derived the magneto-telluric ratios for a fault according to d'Erceville and Kunetz (1959). We have summarized there, only the case where the vertical discontinuity extends from the upper surface through a single layer to the top of a uniform infinitely downward extending lower layer.

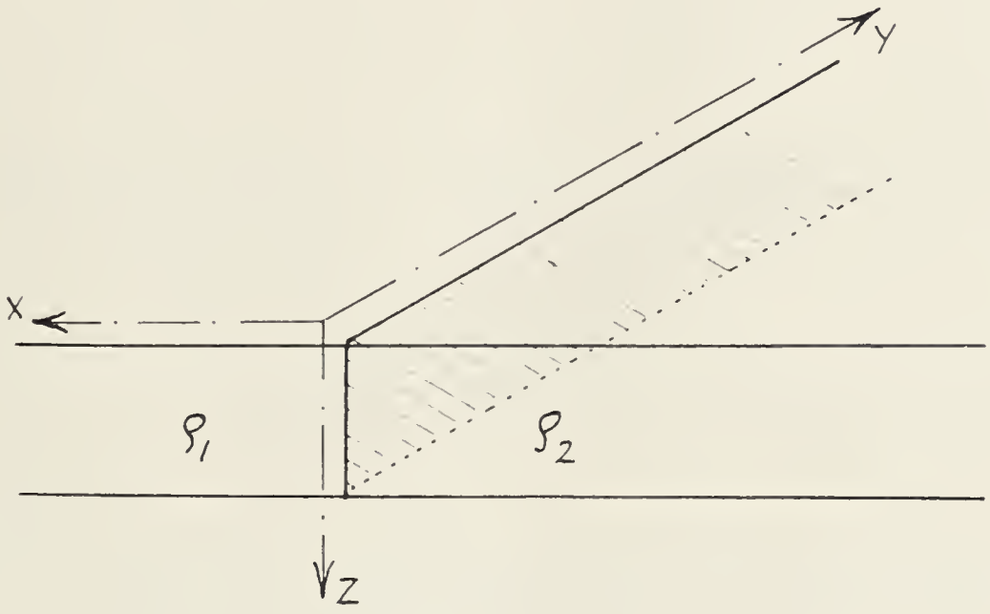


Fig. 8. A fault in a double-layered earth.

The fault surface is the y-z plane at x=0 and extends infinitely in the positive and negative y directions. (Figure 8).

Of at least equal interest to the fault, from a geological-geophysical point of view, is the case of a dike. For this reason it was felt advisable to add to the already existing theory, solutions for some interesting cases of this type.

Consider a dike consisting of two vertical planes infinitely extended in the ± y direction separating a region of resistivity $\rho_1$, from the medium on either side of resistivity $\rho_2$.

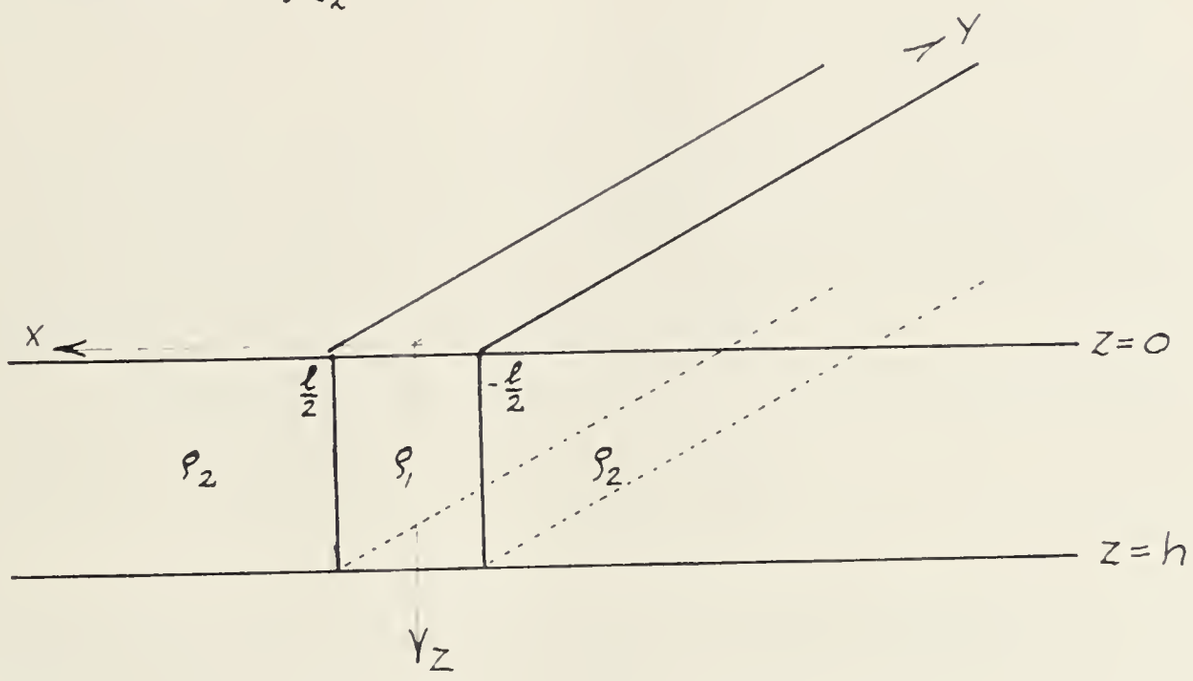


Fig. 9. A dike in a double-layered earth.

We take our origin such that the yz surfaces of discontinuity lie at $x = -\frac{\ell}{2}, \frac{\ell}{2}$. Media (1) and (2) are both underlain by a common infinitely downward extending substratum. (Figure 9).

At large distances from the discontinuity the fields would be those of the appropriate undisturbed double layer. The solutions for these cases are worked out in the Appendix III. The solution for H in the undisturbed region in the medium of resistivity $\rho_1$ will be designated as $H_1$ and that in the medium with $\rho_2$ as $H_2$, bearing in mind that H=Hy. We will now assume that the total solution for the field H is a function of x and z of the form:

$$H(x,z) = H_1(z) + P_1(x,z)$$

in region 1, with a similar expression with subscript 2 in region 2. Each term of this sum must satisfy the propagation equation independently.

We will assume that we can write the disturbance term as the product of two functions:

$$P_i(x,z) = f_i(x)\, g_i(z) .$$

We will further assume that g(z) can be expanded in a Fourier series.

We will consider two special cases:

Case I: Infinitely Resistive Substratum

In Appendix III appear the solutions for a simple double layer of this type. We can observe that the solution $H_1(z)$ vanishes for z=h. Reference to this

appendix will indicate that $H_y(x,z)=H_i(z) + P_i(x,z)$ must also vanish for z=h. Furthermore we have seen in Chapter II that $H_y$ is continuous for z=0 even across the trace of discontinuities in $\rho$. Since P(x,z) is assumed to have no effect for large x we must have that P(x,o)=0. Thus, since P(x,z) is a function which vanishes for z=0 and z=h, we can expand the term g(z) into a sin series of argument $\frac{n\pi z}{h}$ in the interval o,h and include the coefficient of $\sin \frac{n\pi z}{h}$ in the f(x) term.

$$P_i(x,z) = \sum f_{in}(x) \sin \frac{n\pi z}{L} .$$

Each term of this series must satisfy the same propagation equation:

$$\frac{\partial^2 H}{\partial x^2} + \frac{\partial^2 H}{\partial z^2} = 4\pi j\sigma\omega H ,$$

this implies:

$$\frac{d^2 f_{in}(x)}{dx^2} \sin \frac{n\pi z}{h} = \left[\frac{n^2\pi^2}{h^2} + 4\pi j\sigma\omega\right] f_{in}(x) \sin \frac{n\pi z}{h} ,$$

which, after cancelling the common sin term has the solution:

$$f_{in}(x) = a_{in} e^{-K_{in}\frac{x}{h}} + b_{in} e^{K_{in}x}$$

where:

$$K_{in} = \sqrt{n^2\pi^2 + jh_1^2} \quad , \quad h_1 = h\sqrt{4\pi\sigma_1\omega} .$$

This solution satisfies the condition that it vanish for $|x| \to \infty$ if we take only the a-type terms for positive x and only the b-type terms for negative x both in medium 2, while both positive and negative exponentials are permissable in the finite region of medium 1. Symmetry conditions permit us to equate:

$$a_{in} = b_{in}$$

which we observe gives the same value for $H_y(x,z)$ for the same positive and negative values of x. Utilizing the symmetry condition is entirely equivalent to using one of the boundaries for solving for continuity of the field components, only the remaining boundary is now available for solving for the remainder of the coefficients and we write:

$$\sum_{n=1}^{\infty}\left[a_{1n}\, e^{-\frac{k_{1n}\ell}{2h}} + a_{1n}\, e^{\frac{k_{1n}\ell}{2h}} - a_{2n}\, e^{-\frac{k_2\ell}{2h}}\right] \sin\frac{n\pi z}{h} = H_2 - H_1 .$$

If we now expand $H_2 - H_1$ into a sin series of the same argument:

$$H_2 - H_1 = \sum_{n=1}^{\infty} A_n \sin\frac{n\pi z}{h}$$

we can equate, at the boundary, term by term to obtain:

$$2a_{1n}\cosh\left(\frac{k_{1n}\ell}{2h}\right) - a_{2n}\, e^{-\frac{k_{2n}\ell}{2h}} = A_n . \qquad \underline{\text{IV}}-9$$

Recall:

$$E_z = \frac{\rho}{4\pi} \frac{\partial H_y}{\partial x} ,$$

and equating term by term at $x = \frac{\ell}{2}$:

$$2 \frac{\rho_1}{4\pi} \frac{k_{1n}}{h} a_{1n} \sinh\left(\frac{k_{1n}\ell}{2h}\right) + \frac{\rho_2}{4\pi} \frac{k_{2n}}{h} a_{2n} e^{-\frac{k_{2n}\ell}{2h}} = 0 . \quad \text{IV} - 10$$

Solving for $a_{1n}$ from equations (9) and (10):

$$a_{1n} = \frac{A_n}{2\cosh\left(\frac{k_{1n}\ell}{2h}\right) + \frac{k_{1n}h_2^2}{k_{2n}h_1^2} \sinh\left(\frac{k_{1n}\ell}{2h}\right)} \qquad \text{IV} - 11$$

$$a_{2n} = \frac{-A_n \ell \frac{k_{2n}\ell}{2h} \sinh\left(\frac{k_{1n}\ell}{2h}\right)}{\frac{k_{2n}h_1^2}{k_{1n}h_2^2} \cosh\frac{k_{1n}\ell}{2h} + \sinh\left(\frac{k_{1n}\ell}{2h}\right)} . \qquad \text{IV} - 12$$

Following the well known procedure of Fourier series expansion, the coefficient of $\sin\frac{n\pi z}{h}$ in the expansion of $H_2 - H_1$:

$$A_n = \frac{2}{h}\int_0^h \left(H_2 - H_1\right) \sin\frac{n\pi z}{h}\, dz$$

where:

$$H_2 - H_1 = A_2 e^{\sqrt{j}\frac{z}{p_2}} + B_2 e^{-\sqrt{j}\frac{z}{p_2}} - A_1 e^{\sqrt{j}\frac{z}{p_1}} - B_1 e^{-\sqrt{j}\frac{z}{p_1}}$$

$$p_i = \frac{1}{\sqrt{4\pi\epsilon_i \omega}} .$$

Quoting the result of Appendix III, Equations A-3 and A-4:

$$A_i = \frac{H_o e^{-\sqrt{j}\,h_i}}{2\sinh(\sqrt{j}\,h_i)} \quad , \quad B_i = \frac{H_o e^{\sqrt{j}\,h_i}}{2\sinh\sqrt{j}\,h_i} \quad ,$$

from which:

$$A_n = 2\pi j \frac{n H_o (h_1^2 - h_2^2)}{k_{1n}^2 \; k_{2n}^2} \quad ;$$

substituting back into equations (11) and (12) we obtain:

$$a_{1n} = \frac{2\pi j (h_1^2 - h_2^2) a H_o n}{k_{1n}^2 k_{2n}^2 \left[2\cosh\left(\frac{k_{1n}\ell}{2h}\right) + \frac{k_1 h_2^2}{k_2 h_1^2} \; 2\sinh\left(\frac{k_{1n}\ell}{2h}\right)\right]}$$

$$a_{2n} = \frac{2\pi j (h_2^2 - h_1^2) H_o n e^{-\frac{k_{2n}\ell}{2h}} \sinh\left(\frac{k_{1n}\ell}{2h}\right)}{k_{1n}^2 k_{2n}^2 \left[\sinh\left(\frac{k_{1n}\ell}{2h}\right) + \frac{k_{2n} h_1^2}{k_{1n} h_2^2} \cosh\left(\frac{k_{1n}\ell}{2h}\right)\right]} \quad .$$

<u>In medium 1</u>

$$H_y = \frac{H_o}{2\sinh(\sqrt{j}\,h_1)}\left[-e^{-\sqrt{j}\,h_1 + \sqrt{j}\,\frac{z}{P_1}} + e^{\sqrt{j}\,h_1 - \sqrt{j}\,\frac{z}{P_1}}\right] + \sum_{n=1}^{\infty} a_{1n}\, 2\cosh\frac{k_1 x}{h} \sin\frac{n\pi z}{h}$$

$$E_x = \frac{H_o S_1}{+\pi\, 2\sinh(\sqrt{j}\,h_1)}\left[\frac{\sqrt{j}}{F_1} e^{-\sqrt{j}\,h_1 + \sqrt{j}\,\frac{z}{P_1}} + \frac{\sqrt{j}}{F_1} \; \left[\sqrt{j}\,\frac{z}{P_1}\right]\right.$$

$$\left. - \frac{\rho_1}{4\pi} \sum_{n=1}^{\infty} \frac{n\pi}{h} a_{1n}\, 2\cosh\frac{k_{1n}x}{h} \cos\frac{n\pi z}{h}\right] \quad .$$

At the upper surface z = 0, where we measure the magneto-telluric fields $H_y = H_o$

and:

$$\left(\frac{E_x}{H_y}\right)_1 = \sqrt{j}\,\frac{\omega h}{h_1}\coth\left(\sqrt{j}\,\eta_1\right) - 2\pi^2 j\,\frac{\omega h}{h_1^2}\left(h_1^2 - h_2^2\right)U_1$$

where:

$$U_1 = \sum_{n=1}^{\infty} \frac{n^2 \cosh\left(k_{1n}\frac{x}{h}\right)}{k_{1n}^2\, k_{2n}^2\left[\cosh\left(\frac{k_{1n}\ell}{2h}\right) + \frac{k_{1n}h_2^2}{k_{2n}h_1^2}\sinh\left(\frac{k_{1n}\ell}{2h}\right)\right]} \quad .$$

In medium 2

The constant term is the same as for medium 1 with the subscripts interchanged but the disturbance term is:

$$P_2 = \sum_{n=1}^{\infty} a_{2n}\, e^{-\frac{k_{2n}x}{h}} \sin\frac{n\pi z}{h}$$

and the disturbance term for Ex:

$$\left(E_x\right)_2 = \frac{-P_2}{4\pi}\sum_{n=1}^{\infty} a_{2n}\,\frac{n\pi}{h}\, e^{-\frac{k_{2n}x}{h}} \cos\frac{n\pi z}{h} \quad .$$

At the surface where $H_y = H_o$ :

$$\left(\frac{E_x}{H_y}\right)_2 = \sqrt{j}\,\frac{\omega h}{h^2}\coth\left(\sqrt{j}\,h_2\right) - 2\pi^2 j\,\frac{\omega h}{h_2^2}\left(h_2^2 - h_1^2\right)U_2$$

where:

$$U_2 = \sum_{n=1}^{\infty} \frac{n^2 e^{\frac{k_{2n}\ell}{2h}} \sinh\left(\frac{k_{1n}\ell}{2n}\right) e^{\frac{-k_{2n}x}{h}}}{k_{1n}^2\, k_{2n}^2\left[\sinh\left(\frac{k_{1n}\ell}{2h}\right) + \frac{k_{2n}h_1^2}{k_{1n}h_2^2}\cosh\left(\frac{k_{1n}\ell}{2h}\right)\right]} \quad .$$

Case II: Infinitely Conducting Substratum

In Appendix III apear the solutions for a simple double layer of this type. The solution $H_i(z)$ does not vanish for z = h. Thus in the general expression:

$$H(x,z) = H_i(z) + P_i(x,z)$$

$P_i(x,z)$ must vanish for z = 0 for the same reason as in the preceeding example, while at z = h it must have a finite value determined by the continuity of H(x,z) at $x = \pm \frac{\ell}{2}$ . Thus, neither $H_2 - H_1$ nor P can be represented simply by a sin series in the interval 0 to h. For convenience we will develop these functions in a sin series of argument $\frac{n\pi z}{2h}$ , where in order to satisfy the boundary conditions at z = h while vanishing at 0 and 2h we will define:

$$H_2 - H_1 = f(2h-z), \quad h \leq z \leq 2h .$$

Proceeding as in the previous example:

$$P_i(x,z) = \sum f_{in}(x) \sin \frac{n\pi z}{2h} ,$$

each term of which satisfies:

$$\frac{\partial^2 H}{\partial x^2} + \frac{\partial^2 H}{\partial z^2} = 4\pi j\sigma\omega H ,$$

results in:

$$\frac{d^2 f_{in}(x)}{dx^2} = \left[\frac{n^2\pi^2}{4h^2} + 4\pi j\sigma\omega\right] f_{in}(x) ,$$

which has solutions:

$$f_{in} = a_{in} e^{-\frac{k_{in}}{2h}x} + a_{in} e^{\frac{k_{in}}{2h}x} ,$$

where in this case:

$$k_{in} = \sqrt{n^2\pi^2 + 4jh_1^2} ,$$

and we have equated $a_{in} = b_{in}$ for the same reasons as in the previous example. The equations of continuity for $H_y$ and $E_z$ at $x = \frac{\ell}{2}$ result in the same solutions for $a_{in}$ in terms of $A_n$ except that h is replaced by 2 h:

$$a_{1n} = \frac{A_n}{2\cosh\left(\frac{k_{1n}\ell}{4h}\right) + \frac{k_{1n}h_2^2}{k_{2n}h_1^2}\sinh\left(\frac{k_{1n}\ell}{4h}\right)}$$

$$a_{2n} = \frac{-A_n e^{\frac{k_{2n}h_1^2}{4h}}\sinh\left(\frac{k_{1n}\ell}{4h}\right)}{\sinh\left(\frac{k_{1n}\ell}{4h}\right) + \frac{k_{2n}h_1^2}{k_{1n}h_2^2}\cosh\left(\frac{k_{1n}\ell}{4h}\right)} ,$$

noting that in $K_{1n}$ and $K_{2n}$, h is also replaced by 2 h.

When solving for $A_n$ we note that:

$$A_n = \frac{2}{2h}\left[\int_0^h f(z)\sin\frac{n\pi z}{2h}\,dz + \int_h^{2h} f(2h-z)\sin\frac{n\pi z}{2h}\,dz\right]$$

where:

$$f(z) = H_2 - H_1$$

and $H_2$ and $H_1$ are obtained in Appendix III.

$$A_n = 16\pi j H_o(h_1^2 - h_2^2)\frac{2n+1}{k_{1n}^2 k_{2n}^2} ,$$

i.e., only the odd terms of the series appear, therefore we must substitute 2n+1 for n in $K_{1n}$ and $K_{2n}$, with the understanding that n starts at zero instead of at unity.

The complete result for an infinitely conducting substratum is:

$$\frac{E_1}{H_o} = \sqrt{j}\,\frac{\omega h}{h_1}\tanh\left(\sqrt{j}\,h_1\right) - 8\pi^2 j\,\frac{\omega h}{h_1^2}\left(h_1^2 - h_2^2\right) U_1$$

$$U_1 = \sum_0^\infty \frac{(2n+1)^2 \cosh\left(k_1 \frac{z}{2h}\right)}{k_{1n}^2\, k_{2n}^2\left[\cosh\left(\frac{k_{1n}\ell}{4h}\right) + \frac{k_{1n} h_2^2}{k_{2n} h_1^2}\sinh\left(\frac{k_{1n}\ell}{4h}\right)\right]},$$

similarly:

$$\frac{E_2}{H_o} = \sqrt{j}\,\frac{\omega h}{h_2}\tanh\left(\sqrt{j}\,h_2\right) - 8\pi^2 j\,\frac{\omega h}{h_2^2}\left(h_2^2 - h_1^2\right) U_2$$

$$U_2 = \sum \frac{(2n+1)^2 e^{\frac{k_{2n}\ell}{4h}} \sinh\left(\frac{k_{1n}\ell}{4h}\right) e^{-\frac{k_{2n}x}{2h}}}{k_{1n}^2 k_{2n}^2\left[\sinh\frac{k_{1n}\ell}{4h} + \frac{k_{2n} h_1^2}{k_{1n} h_2^2}\cosh\left(\frac{k_{1n}\ell}{4h}\right)\right]}$$

$$k_{1n} = \sqrt{(2n+1)^2 + 4j h_i^2}\,.$$

Presentation of Data and Interpretation for Faults and Dikes

The records of a magneto-telluric traverse will in general contain a broad band of frequencies recorded at each station. While a frequency analysis and interpretation may be attempted at an individual station, using the methods outlined in Chapter III, such a

procedure could lead to erroneous conclusions if it were based on an assumption of a layered sedimentary basin. It would be more meaningful to construct and analyze profiles at discrete frequencies. These profiles would be obtained by plotting the amplitudes and phase angle respectively for the appropriate station co-ordinates. Because of the large contrast in resistivity, and hence magneto-telluric response, it is useful to plot the amplitudes of $\frac{E}{H}$ as a logarithmic ordinate. However, for obvious reasons, positions, regardless of the units chosen, must be plotted on a linear scale.

The theoretical expressions for the magneto-telluric ratio become increasingly complex as the number of interfaces is increased, even for a simple layered system. When there are vertical discontinuities it is easily seen that it is no longer possible to represent the totality of magneto-telluric soundings by a single family of curves, as in the case of the one interface of the two-layered system.

The interpretation for the case of a fault as discussed by d'Erceville and Kunetz (1959) illustrates the order of the increase in the number of families of curves required for a complete interpretation. The addition of a second vertical interface for the dike adds another parameter, namely "$\ell$" the width of the dike, and hence another order of families of curves.

We will restrict our efforts, and those of the University of Alberta computing centre, for the most part to the construction of those curves from which we can attempt to interpret our experimental data.

It can readily be seen that the first term in the theoretical expressions for $\frac{E}{H}$ is just the result one obtains for the undisturbed double-layer cases of Appendix III. The summation for region 2 which lies outside the dike, converges very rapidly for $\frac{x}{h}>0$ and indeed is virtually zero for x=h. Thus one can use the method of interpretation of Chapter III to solve for $\rho_2$ , and h from the spectrum of frequencies, at stations sufficiently far removed from the disturbing boundary. In this case $\rho_2$ refers to the resistivity of the upper layer. Within the dike the range of $\frac{x}{h}$ may be very restricted and hence one is in general unable to solve for $\rho_1$ as in the case of $\rho_2$.

In the summation term the multiplying factor, besides constants, contains parameters in the following combination:

$$\omega h\left[\frac{h_1^2-h_2^2}{h_1^2}\right] = \omega h\left[1-\frac{\rho_1}{\rho_2}\right]$$

for the region inside the dike, and:

$$\omega h\left[1-\frac{\rho_2}{\rho_1}\right]$$

for the region outside the dike. We have plotted

$\frac{E}{H}$ versus the ratio $\frac{x}{h}$ for the various values of the ratio $\frac{\rho_2}{\rho_1}$ and of h and $\ell$ which have been used in the model. We have transformed our data into the "practical" system of units for this purpose. The theoretical and experimental results will be described and discussed in the next chapter.

The theoretical results obtained by d'Erceville and Kunetz (1959) for the fault, indicate certain features of interest which may be applicable also to the dike. Some computed curves for this case will be shown in Figures 12 and 13, Chapter VII. Besides the expected result that at long distances from the discontinuity $\frac{E}{H}$ has the value appropriate to the undisturbed layered system, is the interesting result that the ratios of the values of $\frac{E}{H}$ on adjacent sides of the discontinuity are just the ratios of the D.C. values of $\rho$ .

The aforementioned appropriate value of $\frac{E}{H}$ at remote distances depends on two factors in addition to the resistivities of the upper layer. The resistivity of the substratum, and the period, can dominate the behaviour of $\frac{E}{H}$ for all positions measured.

The curves of Figures 12 and 13 illustrate the remarkable effect of the substratum for longer periods. It can be seen that the curves labeled A are flat right up to the discontinuity on both sides, whereas curves

B display large variations near the interface. For the former case it can be seen that only at the highest frequency used and then only in the region of lowest resistivity of the upper layer, is there a beginning of a departure from a constant value.

# CHAPTER V

## THE REAL EARTH AND THE LABORATORY MODEL

One of the difficulties involved in the measurement of natural electro-magnetic fields is the extremely complex nature of the earth's electrical properties. Some values for resistivity are shown in Table 3 from Rooney (1939):

| Media | Ohm-meters |
|---|---|
| Clays, dense alluvia, etc. ..... | 1 to 30 |
| Sedimentary rocks, new ..... | 10 to 300 |
| Sedimentary rocks, old ..... | 300 to 2,000 |
| Igneous rocks ..... | 500 to 5,000 |
| Coarse gravel, sand, etc. ..... | 750 to 50,000 |

Table 3 Resistivity of Various Earth Constituents

According to the method of interpretation discussed previously, it should be possible to ignore relatively thin layers of highly conducting materials and correspondingly thicker layers of less conducting materials in the event that the appropriate range of frequencies is chosen. In the earth an upper layer of sedimentary rock which may be as thick as 10 km is underlain by a

granitic layer to a total depth of 30 to 40 km. It can be seen from the table that the resistivities of these two layers overlap, hence they could be considered as a single layer underlain by a basaltic layer of resistivity $10^5$. Computations as reported by McNish (1939) give a value of 10 ohm-meters to a depth of 100 km with indications that below that the resistivity is 1 ohm-meter. It is obvious that these values do not compare with any of the known values as given above and must then be the effect of a highly conducting region corresponding to a depth penetrated by the twenty-four hour diurnal variation. The vertical discontinuities can be more pronounced and closer to the surface. A survey of the available data illustrates the severe restrictions on the possible materials suitable for the construction of a scale model, bearing in mind that the scale factors must satisfy the relationship,

$$K_\ell^2 = K_\rho K_t \ .$$

Apart from solutions the only homogeneous conducting materials are graphite and the metals, both of which would require inconveniently small models, and hence impossibly severe restrictions on the size of probe spacing and magnetic detectors. From among the solutions we chose that of ordinary NaCl, since it has a reasonably low

resistivity in concentrated form and it has a relatively slow reaction rate with certain useful metals. The temperature coefficient of resistivity is also quite reasonable for use in an open room. The resistivity of the concentrated salt solution at $22^{o}$ C. is $4 \times 10^{-2}$ ohm-meters. The salt solution provides a uniform single layer which is in our laboratory, underlain by a small depth of a dielectric and then by concrete floor underneath which are metallic conduit and pipe. The details of the model are given in the next section. For a dike we have used graphite which gives, even with the concentrated solution, an extreme contrast from a geological point of view. We have taken advantage of the assumed behavious of thin layers of very highly conducting material to separate solutions of different concentration and hence conductivity as was discussed in Chapter II.

This has allowed us to simulate dikes and faults of moderate resistivity contrast. The details of these model structures will be discussed in the next chapter.

Another major problem of field measurements, that of suitably recording low amplitude, low frequency signals against a persistent background of higher frequency diurnal variations, is being attacked from an instrumental point of view, as is the equally formidable problem of

resolving the various frequency components, on the records, for analysis. A laboratory model avoids this complication, since in the experiment one has control not only of the set of discrete frequencies one wishes to use, but also of the geometry and thus the direction of polarization. The possibility of anisotropic resistivity variations, which have been discussed by Cantwell (1960), can add considerably to the difficulties of both field and laboratory studies.

While a model study can greatly simplify certain aspects of the problem, especially in verifying theoretical solutions, there are special problems in electromagnetic modeling, in addition to those which plague all other model studies. These problems arise due to the coupling of remote objects with the model through the electro-magnetic field. In this way end effects are far more severe than in the electro-static case, for example. Radio stations and beacons can be quite readily detected. Methods of reducing this latter effect without recourse to filtering will be described in the next chapter. The effect of unwanted conductors, some of which are also magnetic, is a problem of the laboratory in which the experiment is carried out. In our laboratory the conduit and service pipes under the floor provided the most serious problem in that it is no longer permissible to

speak of a simple two-layered problem in the discussion of our model.

In order to appreciate the effect of the finite dimensions of the tank, consider a conducting medium threaded by an alternating magnetic field. The induced electric field will cause a current to flow, and if the medium is finite in length in the direction of the current, charge will pile up in such a way as to partly neutralize the field.

Preliminary measurements in our model indicated that the magnitude of the magneto-telluric ratios were many orders of magnitude too small to verify the theory for a layered earth. In addition, the magnitude of E was so small that the probe spacing was of necessity made too large to bring out the details of the effect of vertical dikes or faults. We were in fact measuring average fields over distances which covered the whole range of variations.

Since our major purpose was to investigate the effect of vertical discontinuities we adopted certain modifications to our model in an endeavour to allow the use of smaller probe spacing and to diminish the end effects. These modifications are discussed in detail in the next chapter.

# CHAPTER VI

## APPARATUS AND PROCEDURE

The magnetic field was generated by a current which was as large as 60 amperes, flowing in a rectangular loop constructed of ½" x 1/8" copper bus bar. (Figure 10). The power was supplied by a McIntosh 60-watt audio-amplifier matched to the loop by a step-down transformer with a single turn secondary. The audio-oscillator, power amplifier and frequency counter are shown in Figure B. The turns ratio could be adjusted from 4:1 to 40:1 in discrete steps. The loop, with dimension 3m x 6m, lay in a vertical plane with the nearest long side 50cm above the centre line of a flat wooden tank. (Figure C). This centre line was the x axis of our co-ordinate systems and was parallel to the current flow in the long sides of the loop. The tank contained a salt solution which acted as the conducting upper layer of our model. Dikes and faults lay with their strikes perpendicular to the x axis, i.e. in the direction of the magnetic field. The tank had a length of 2m and a width of 1½ m.

Preliminary measurements indicated that the end effects were extremely pronounced. The $\frac{E}{H}$ ratio was many orders of magnitude too small, while at the same

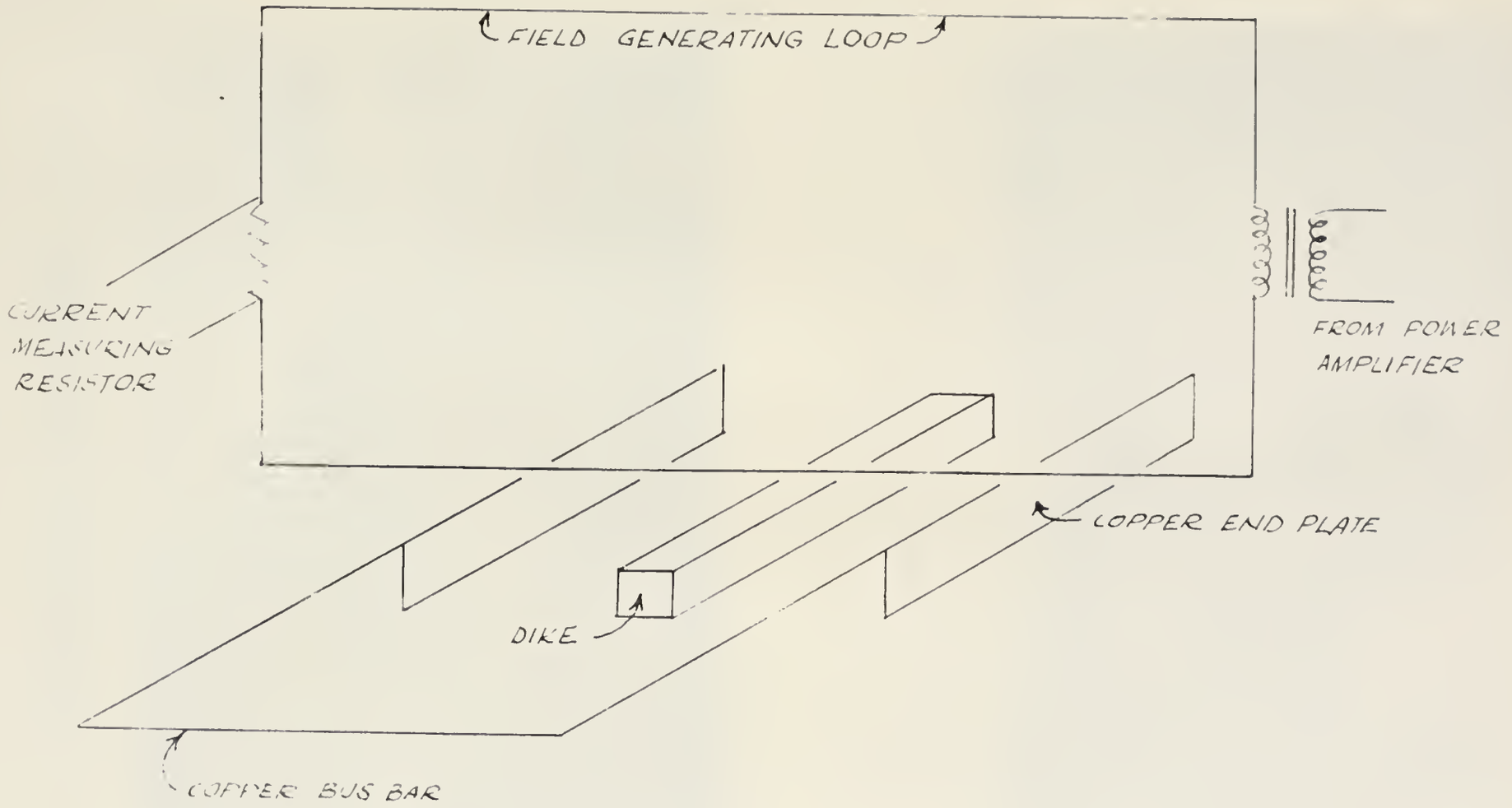


Fig. 10. Schematic diagram of general experimental arrangement.

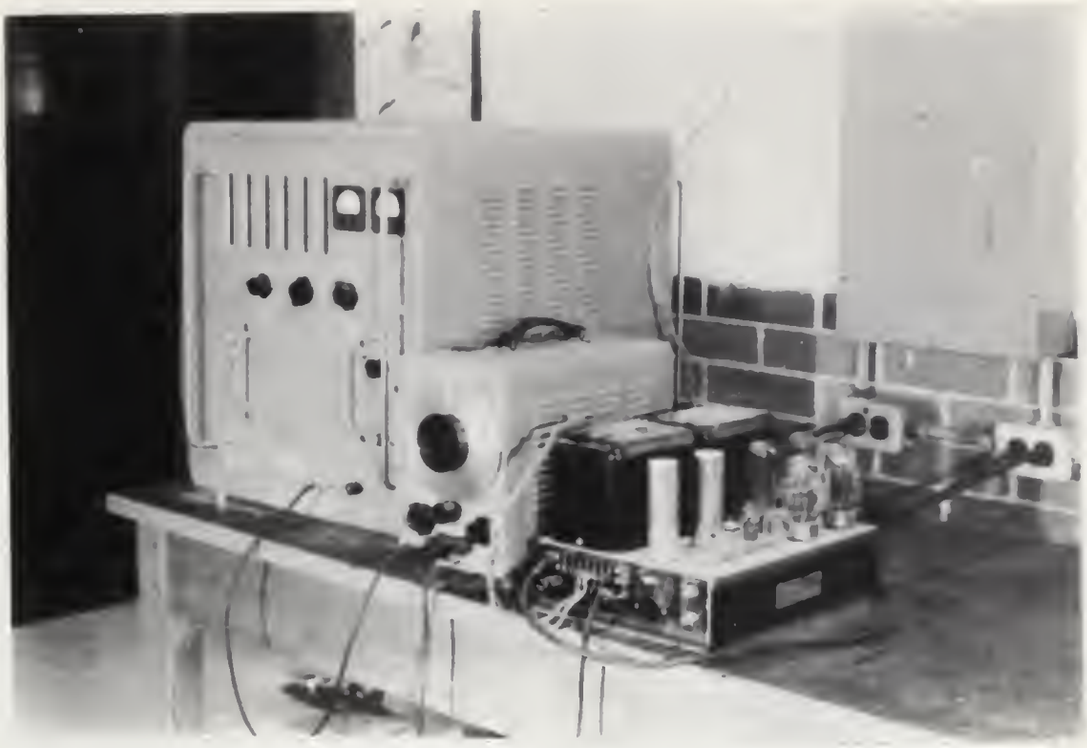

Fig. B. Instrument section; audio-oscillator, power amplifier, and frequency counter.

Fig. C. Wooden tank, containing layer of solution and graphite dike.

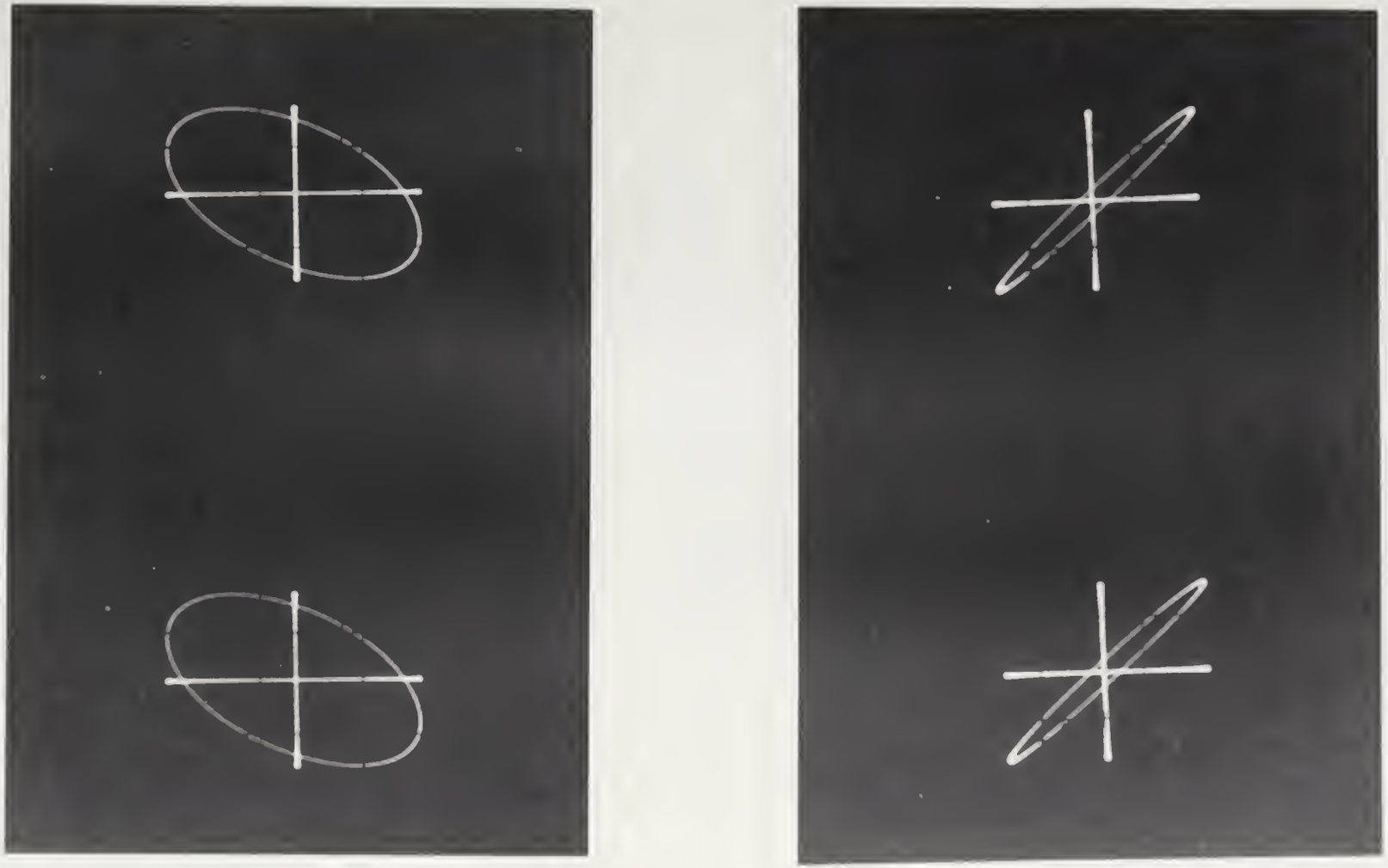

Fig. D. Photographs of signals on oscilloscope screen.

time the ratio varied by over 7% in a traverse of ± 50 cm from the centre of the tank and this effect increased radically as the ends were approached more closely.

We have attempted to improve our model by placing copper sheets at each end of the tank and shorting them together with the bus bar. This bus bar is led out at right angles to the current flow and joined 2½ meters away at the wall of the laboratory (Figure 10), in order to minimize the interaction of the current in this part of the circuit with the current in the conducting solution. The resulting E.M.F. induced in this loop did not appear to affect the measurements too seriously. The uniformity of the field along the x axis was greatly improved while the $\frac{E}{H}$ ratio appeared to be of the right order of magnitude.

The measurement of the magnetic field was accomplished by using a pick-up coil, previously calibrated in terms of the free space response of the coil with respect to the computed magnetic field at the centre of a circular loop.

The electric field was derived from the voltage drop between two probes separated by a distance of 2 cm along the x axis. It is thus the average field which was measured, over a distance which was made as short as

feasible. In actual practice a third probe was introduced which was connected to the centre tap of the measuring instrument, in our case, a Techtronix 502 oscilloscope. In this way our measurement of E is:

$$E = \frac{V_b - V_a}{b-a} = \frac{(V_b - V_g) - (V_a - V_g)}{b-a}$$

where $V_g$ is the voltage to ground.

Both the magnetic and electric signals appeared in turn as the vertical component of a Lissajous figure on the screen of the oscilloscope, the horizontal component being a reference signal which was measured as the voltage drop across a non-inductive element of the source loop. The measured and computed resistance of this element was $4.84 \times 10^{-4}$ ohms.

The third probe was introduced into the electric field measuring system in order to cancel out that part of the noise which affected both probes alike. This function it performed most efficiently; the noise, which appeared when an attempt was made to measure simply $V_a$-$V_g$, was many times larger in magnitude than the signal level, but could be reduced to tolerable levels when the differential probe system was used. That part of the noise which was directional and had a component in the x direction could not be so eliminated. Our conducting layer was apparently an efficient "aerial" for radio

frequencies which were radiated upward through the floor. This high frequency noise which modulated all electric signals could be "stopped" in a visual presentation on the oscilloscope. The tuning requirement was too exacting to allow a photograph to be taken of the modulated signal and in general this noise merely produced a line broadening. It was felt, however, that the signal to noise ratio was adequate without the use of filters. The magnetic pickup was not as susceptible to noise since its response was peaked in the audio range of frequencies.

Both the electric and magnetic signals were photographed on Polaroid film. The lens gave a 1:1 image of the oscilloscope screen, the oscilloscope itself being previously calibrated. Triple exposures were made to facilitate the measurement of the horizontal and vertical amplitudes and the intercepts, each individually. Sample photographs appear in Figure D.

In order to simulate a fault, a tray, one end of which is a thin copper plate, is placed in the tank, the copper plate then separates a region containing a concentrated salt solution of resistivity $4 \times 10^{-2}$ ohm-meters from a region containing a dilute salt solution of resistivity .71 ohm-meters. The depth of the layer was 20 cm in this case.

In the case of the dike, a tray of length 10 cm with copper plates on both ends was used. Two situations were examined; the one in which the dike contained the concentrated, more highly conducting solution, in an environment of the less conducting solution; and the situation with the solutions interchanged.

While it is assumed that it is permissable to neglect the effect of thin metallic conductors where the current and electric field lines are normal to the metallic surface, it is not permissable to introduce such conducting material which provides conducting paths parallel to this field direction. Hence, in order to study discontinuities lying at depth, it is necessary to use some other device, than surrounding a solution with a metallic conductor. Two solid dikes were used, extending 10 cm in the x direction as in the previous cases but of half the depth. This would correspond to a large depth of burial in the real earth, depending on the frequency employed. A graphite dike provided a sharp low resistivity contrast and a block of concrete encased in wood provided a sharp high resistivity contrast, in each case compared to both a concentrated and dilute salt solution.

For comparison, traverses were run on these same dikes in a shallow layer of the concentrated solution.

In this case, 2 mm of the solution overlay the dikes in order for the electric probes to make contact.

The results and interpretation for all these cases, as well as various magneto-telluric soundings on the Cagniard system will be discussed in Chapter VII.

# CHAPTER VII

## RESULTS, INTERPRETATION, AND CONCLUSIONS

In our calculations for the theoretical curves, we have employed the actual dimensions, frequencies and resistivities which were used in the experiment. To these "real" measurements correspond an infinite number of "models" of earth size dimensions, according to the scaling factors we choose for any pair of the parameters; the third parameter being determined through the relationship:

$$K_\ell^2 = h_\rho K_t .$$

In Table 4 are shown several possible geological situations corresponding to the several examples selected from among our measurements.

### Frequency Analysis of the Layered Earth

In the two-layered earth case it can be observed that at the shortest period used, the upper layer thickness was less than one skin depth. According to the method of interpretation discussed in Chapter III for a simple layered earth, it is shown that for sufficiently short periods, the apparent resistivity approaches the resistivity of the upper layer, or

| CASE | LABORATORY DIMENSIONS | SCALE FACTORS | GEOLOGICAL DIMENSIONS |
|---|---|---|---|
| Two-layered earth | $h = 2 \times 10^{-4}$<br>$\rho_1 = 4 \times 10^{-2}$<br>$T = 9 \times 10^{-6}$ to $36 \times 10^{-4}$ | $K_\ell = 10^4$<br>$K_\rho = 10^4$<br>$K_T = 10^4$ | $h' = 2$ KM<br>$\rho_1' = 400$ ohm-meters<br>$T' = .09$ to 36 sec. |
| | ..... | | |
| Fault | $h = 2 \times 10^{-4}$<br>$\rho_1 = 4 \times 10^{-2}$<br>$\rho_2 = 7.1 \times 10^{-1}$<br>$T = 16 \times 10^{-6}$ | $K_\ell = 10^4$<br>$K_\rho = 10^4$<br>$K_\rho = 10^4$<br>$K_t = 10^4$ | $h' = 2$ Km<br>$\rho_1' = 400$ ohm-meters<br>$\rho_2' = 7100$ ohm-meters<br>$T' = .16$ sec. |
| | ..... | | |
| Dike | $h = 10^{-4}$<br>$\ell = 10^{-4}$<br>$\rho_1 = 8 \times 10^{-6}$<br>$\rho_2 = 4 \times 10^{-2}$<br>$T = 16 \times 10^{-6}$ | $K_\ell = 2 \times 10^3$<br>$K_\ell = 2 \times 10^3$<br>$K_\rho = 2 \times 10^3$<br>$K_\rho = 2 \times 10^3$<br>$K_t = 2 \times 10^3$ | $h' = 200$ m<br>$\ell' = 200$ m<br>$\rho_1' = 1.6 \times 10^{-3}$<br>$\rho_2' = 800$ ohm-meters<br>$T' = .032$ sec. |

TABLE 4

EXTRAPOLATION OF MODEL TO GEOLOGICAL DIMENSIONS

phrasing it more simply, the skin depth is such that the fields virtually do not penetrate the lower layer.

In Figure 11 are shown the results of plotting from the measurements made on the two-layer model:

$$\rho_a = .2T\left|\frac{E}{H}\right|^2$$

to the same scale as the master curves of Figure 5. These curves are extrapolated to shorter periods to indicate their possible asymptotic approach to the value of resistivity measured in a DC conductivity cell.

At the longer period end it can be seen that in the three cases presented, the apparent resistivities coincide. For these very long periods we are essentially measuring the common resistivity of a lower, relatively higher conductivity medium. We could estimate

$$\rho < 10^5 .$$

We have superimposed on these experimental curves segments of the master plot for the two-layer case. It will be recalled from the discussion on interpretation in Chapter III how a three-layer curve can be accurately derived in certain cases as a composite of two-layer segments. Under less restrictive conditions a composite curve can indicate qualitative aspects of a more general layered earth.

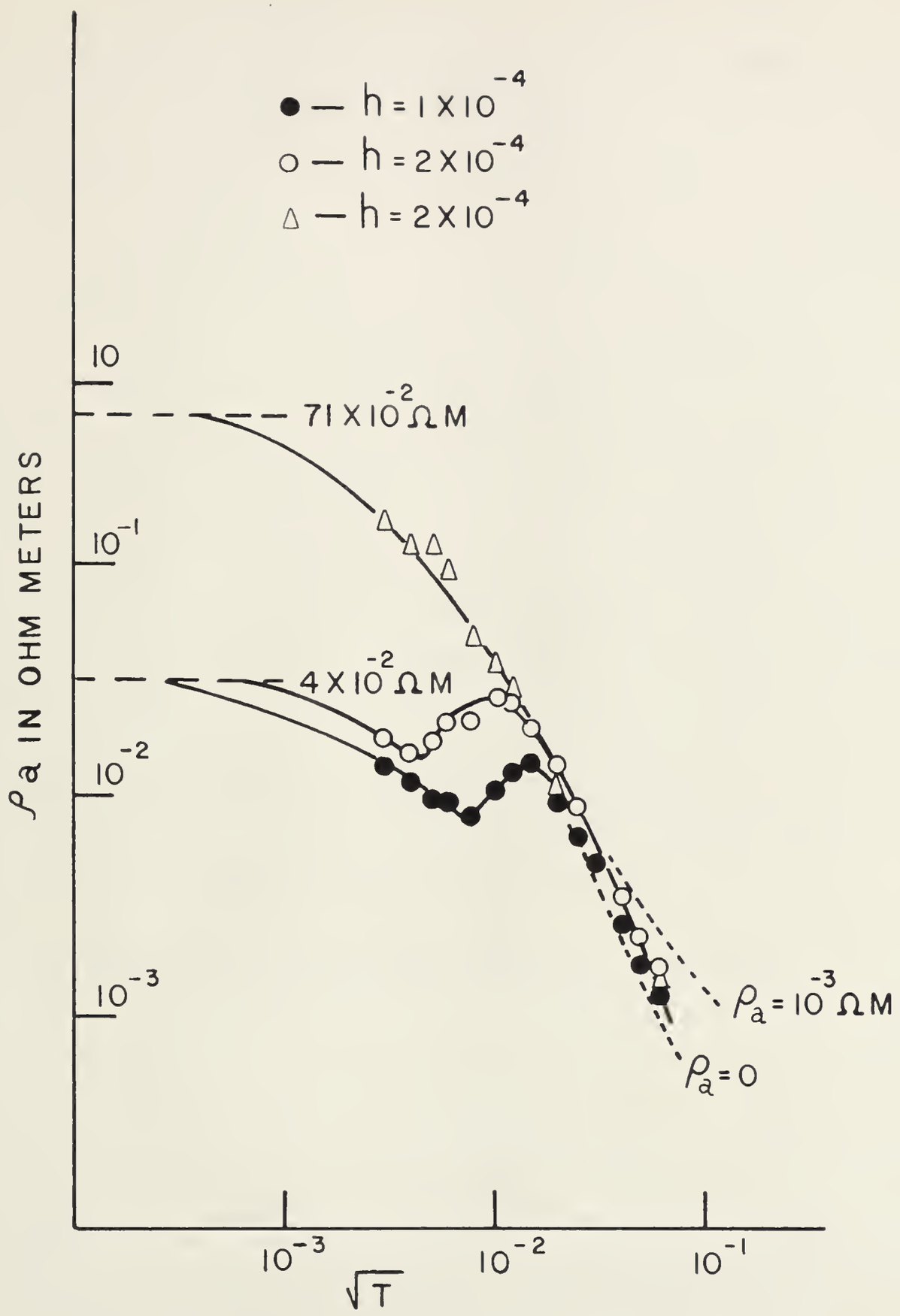


Fig. 11. Frequency analysis for a simple conducting layer measured in the tank.

We interpret the results plotted in Figure 11 as indicating that the relatively thin upper layer of our model is underlain by an extremely thin layer of more highly resistive material, which is underlain, in turn, by a relatively thick layer of highly conducting material. Keeping in mind that relative thickness is in terms of skin depth, one can see that a few millimeters of a conducting metal can be much thicker for our purposes than a few meters of concrete. Our model is in reality a complicated multi-layered system. The salt solution is in a wooden tank, for all practical purposes an extremely thin layer of dielectric, which in turn rests on an uneven concrete floor, thus there are also air gaps. Imbedded in the concrete is the usual structural steel and beneath that, more concrete, service pipes, conduit, and earth. A quantitative analysis of this arrangement was not considered.

Discussion of Theoretical Results for the Dike

In Figures 12 -to- 17, are plotted the theoretical curves for faults and dikes with the parameters as listed in Table 5. The experimental results for these cases are also plotted on the same figures. The computations which have been completed by the computing centre to date, have parameters selected to fit the experimental data. Even at the highest frequency used, the periods are

| Figure No. | Curve No. | Type of Structure | h | T | $\rho_1$ | $\rho_2$ | $\rho_3$ |
|---|---|---|---|---|---|---|---|
| 12 | A | Fault | $2 \times 10^{-4}$ | $1.6 \times 10^{-5}$ | $4 \times 10^{-2}$ | $71 \times 10^{-2}$ | $\infty$ |
| | B | " | " | " | " | " | 0 |
| | | | ..... | | | | |
| 13 | A | Fault | $2 \times 10^{-4}$ | $3.6 \times 10^{-3}$ | $4 \times 10^{-2}$ | $71 \times 10^{-2}$ | $\infty$ |
| | B | " | " | " | " | " | 0 |
| | | | ..... | | | | |
| 14 | A | Dike | $2 \times 10^{-4}$ | $1.6 \times 10^{-5}$ | $4 \times 10^{-2}$ | $71 \times 10^{-2}$ | $\infty$ |
| | B | " | " | " | " | " | 0 |
| | | | ..... | | | | |
| 15 | A | Dike | $2 \times 10^{-4}$ | $3.6 \times 10^{-3}$ | $4 \times 10^{-2}$ | $71 \times 10^{-2}$ | $\infty$ |
| | B | " | " | " | " | " | 0 |
| | | | ..... | | | | |
| 16 | A | Dike | $2 \times 10^{-4}$ | $1.6 \times 10^{-5}$ | $71 \times 10^{-2}$ | $4 \times 10^{-2}$ | $\infty$ |
| | B | " | " | " | " | " | 0 |
| | | | ..... | | | | |
| 17 | A | Dike | $2 \times 10^{-4}$ | $3.6 \times 10^{-3}$ | $71 \times 10^{-2}$ | $4 \times 10^{-2}$ | $\infty$ |
| | B | " | " | " | " | " | 0 |
| | | | ..... | | | | |

TABLE 5

PARAMETERS OF COMPUTED CURVES PLOTTED IN FIGURES 12 to 17.

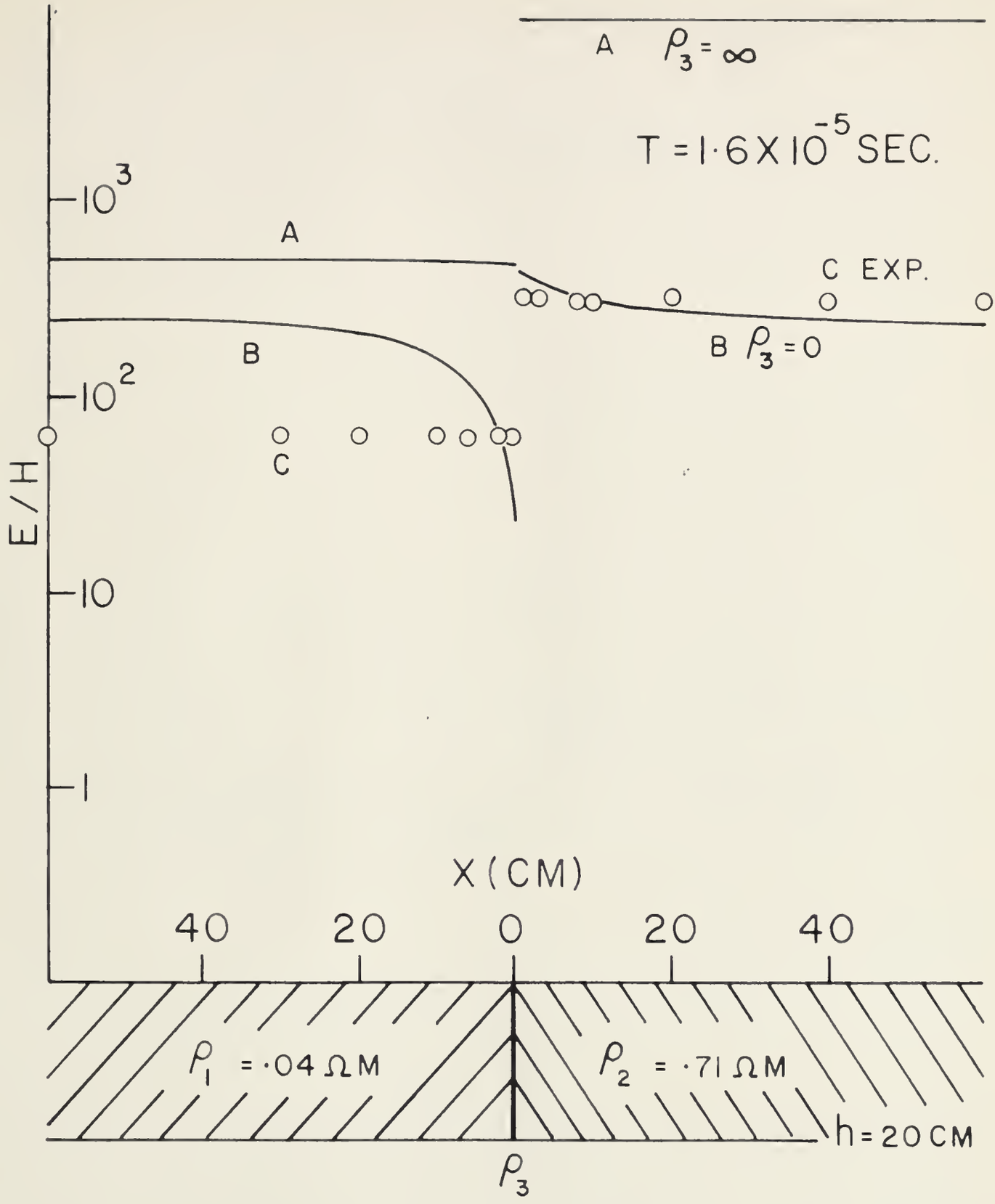


Fig. 12. Computed and experimental values of magneto-telluric ratio over a fault at the higher frequency.

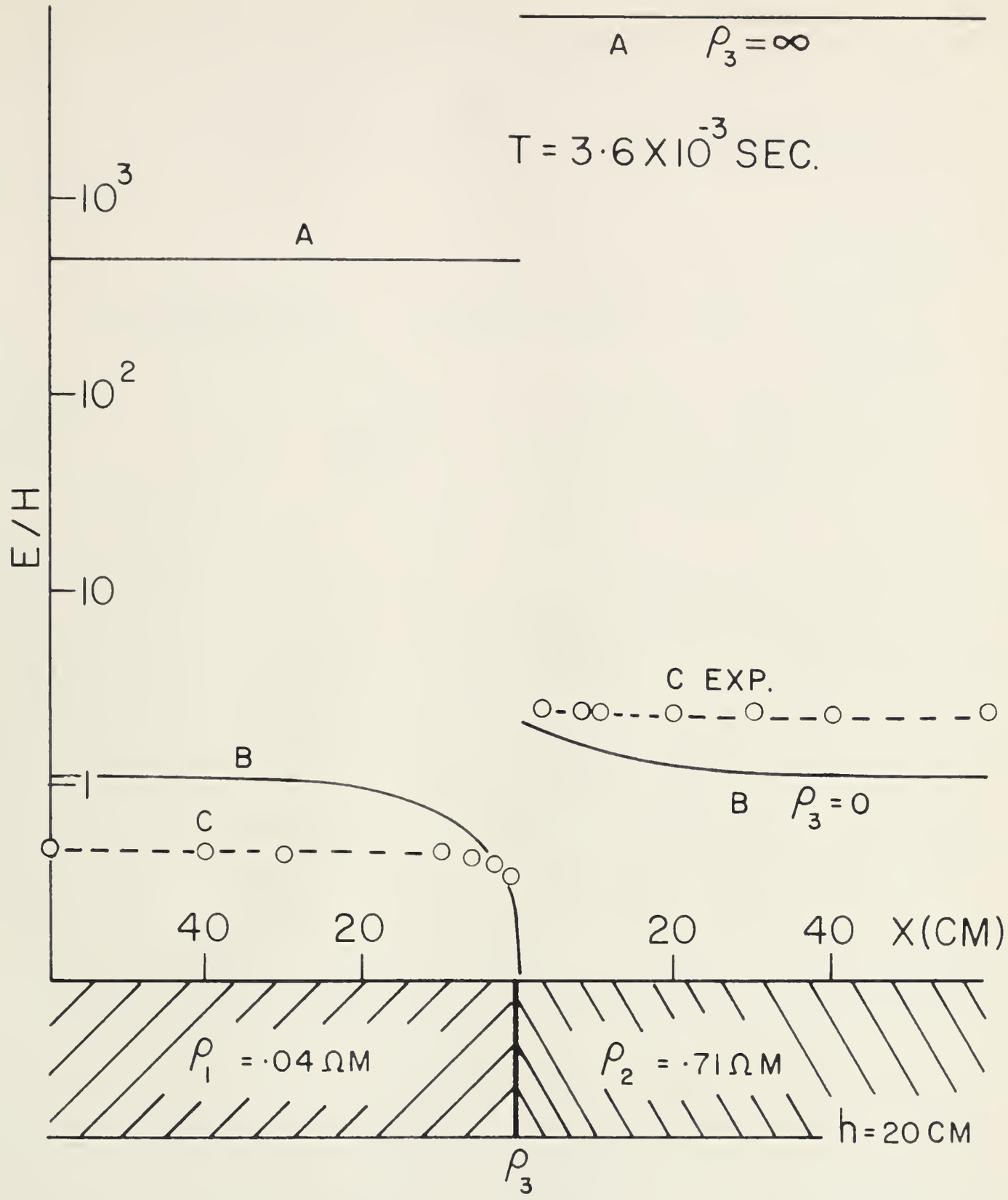


Fig. 13. Computed and experimental values of magneto-telluric ratio for a fault at the lower frequency.

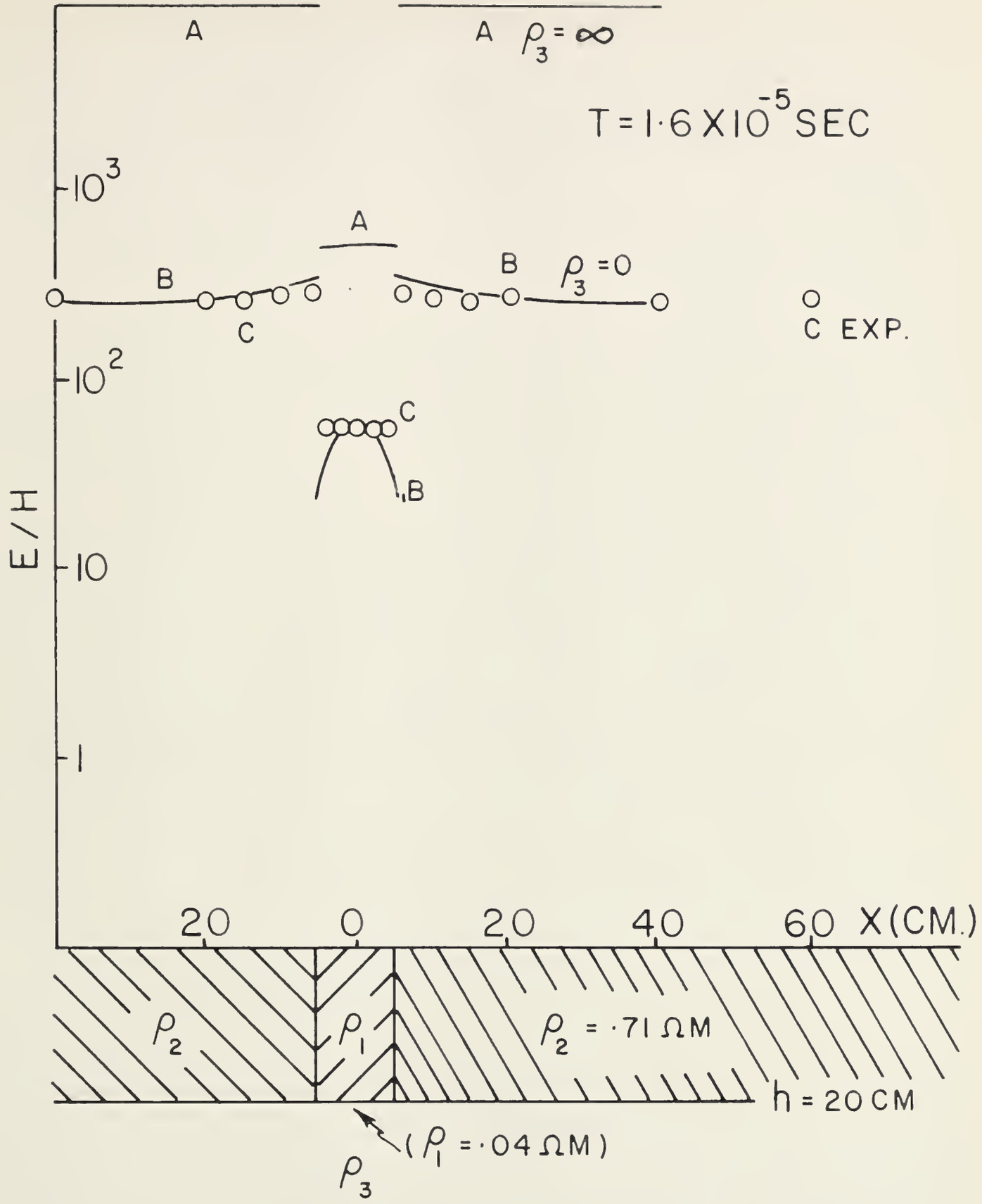


Fig. 14. Computed and experimental values of the magnetotelluric ratio for a conducting dike at the higher frequency.

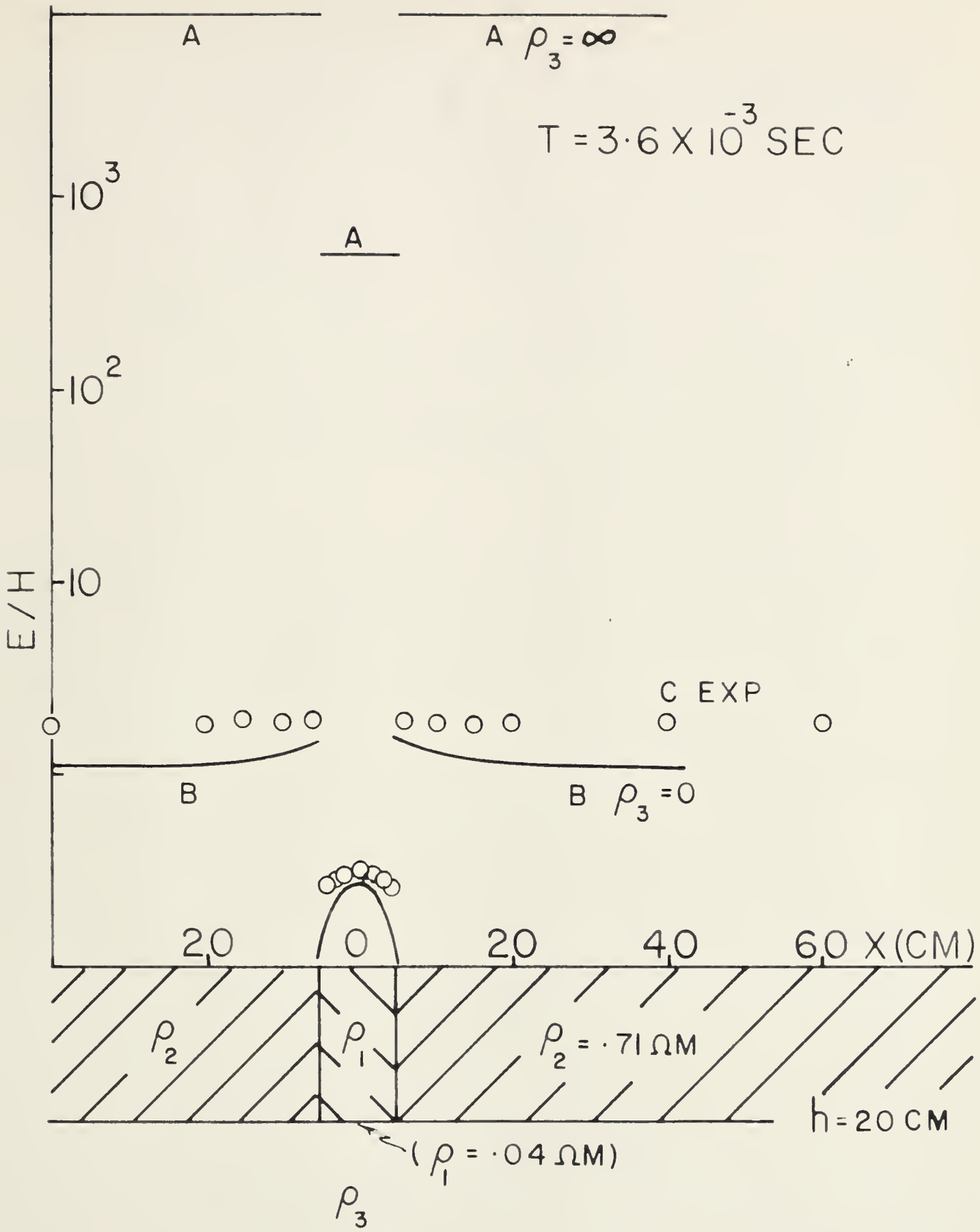


Fig. 15. Computed and experimental values of the magneto-telluric ratio for a conducting dike at the lower frequency.

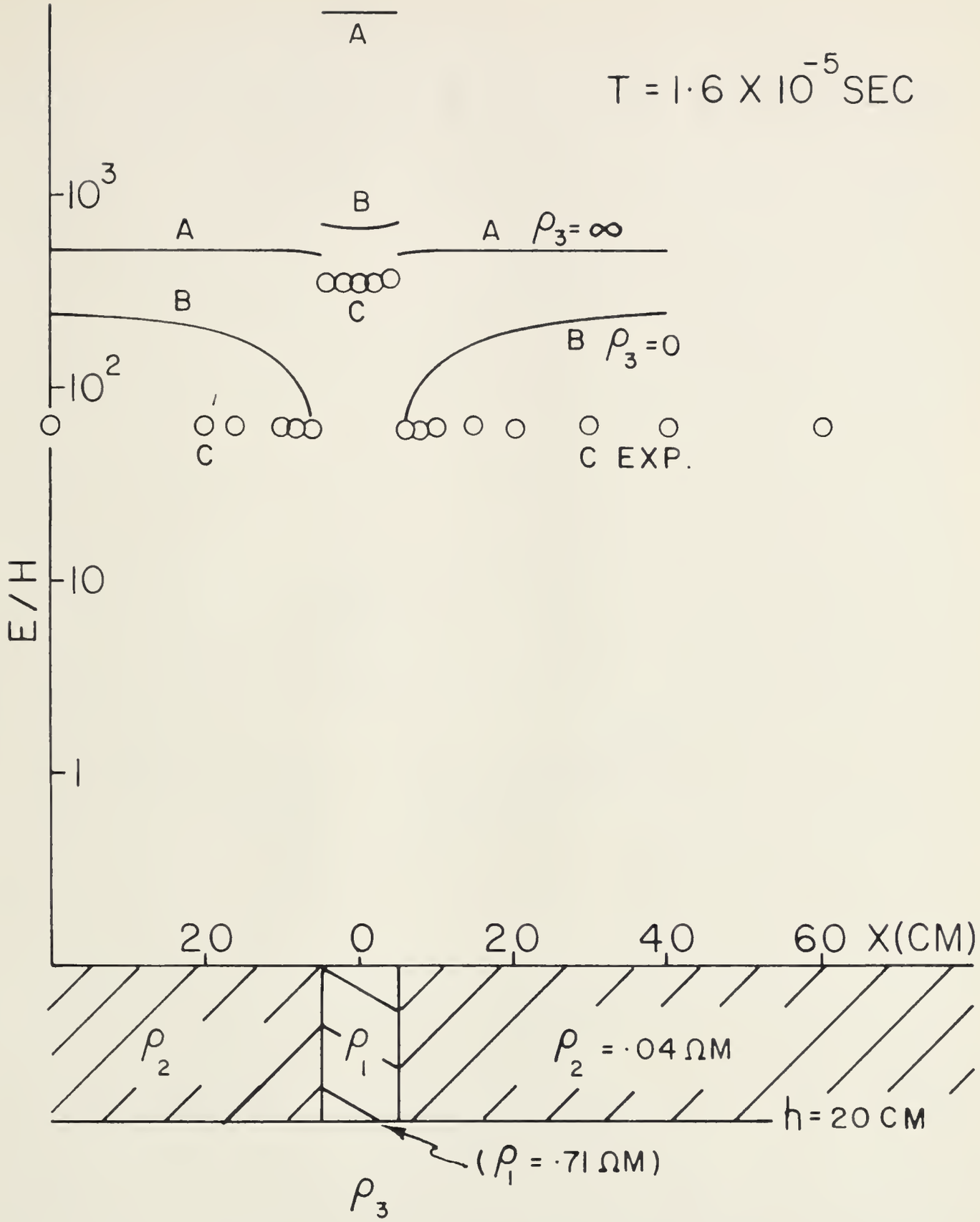


Fig. 16. Computed and experimental values of the magneto-telluric ratio for a resistive dike at the higher frequency.

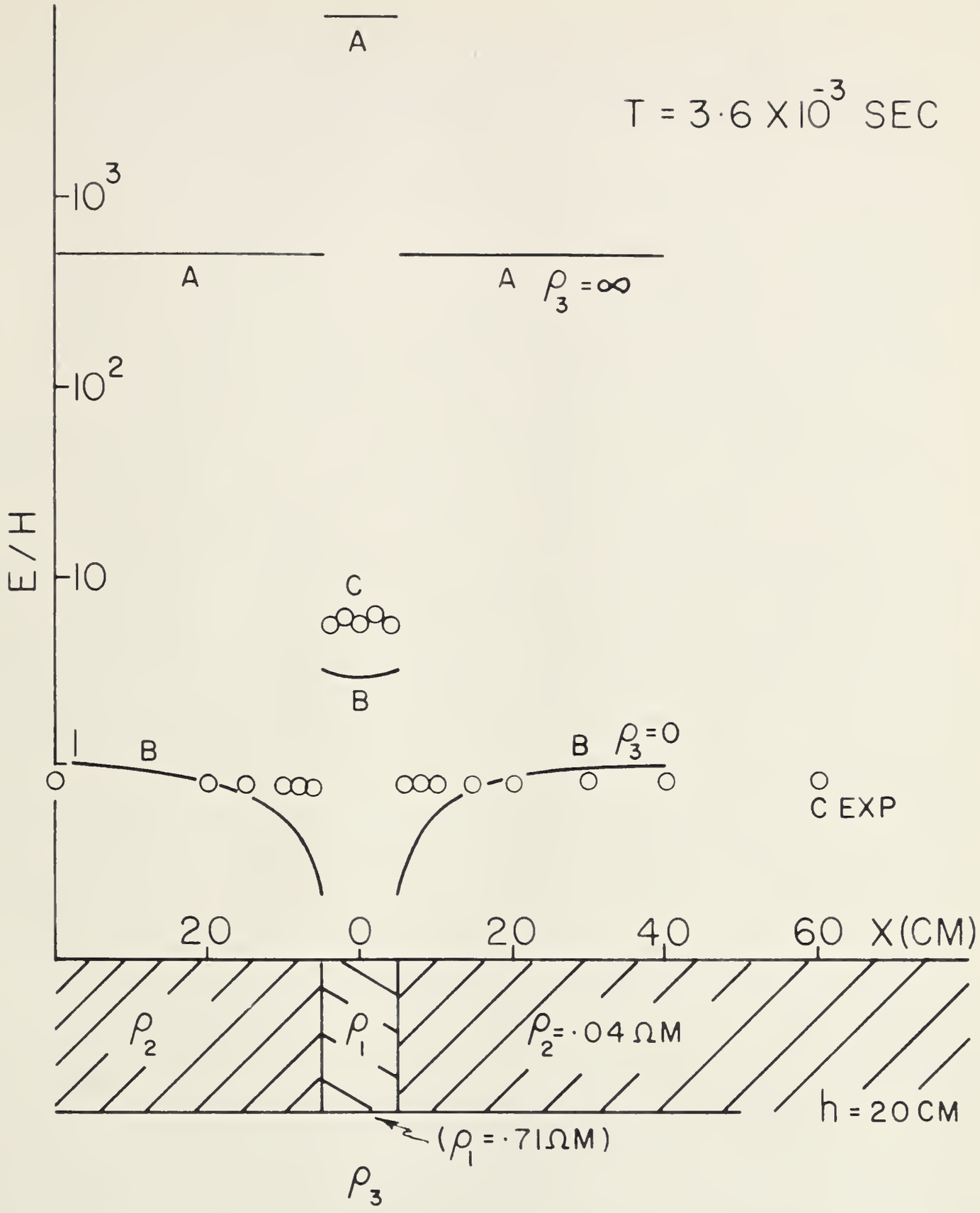


Fig. 17. Computed and experimental values of the magneto-telluric ratio for a resistive dike at the lower frequency.

inconveniently long for a complete interpretation. Computation is continuing at the present time in order to remedy this situation.

Even so, certain marked features can be observed. In direct contrast to the case of the fault, it is possible to have the ratio of $\frac{E}{H}$ on the adjacent sides of a dike interface differ from the DC case. For long periods two possibilities exist. For an infinitely resistive substratum, the situation is dominated by the substratum and the discontinuity in $\frac{E}{H}$ is the same as that of the DC case at each interface. For an infinitely conducting substratum, the discontinuities themselves seem to dominate the situation and $\frac{E}{H}$ at one interface is affected to some extent by the more distant interface.

For shorter periods the situation is more complex. In addition to the effect of either, or both, of the horizontal and vertical interfaces, there is the effect in the upper layers of the skin depth.

The curves of Figures 12 through 17 indicate that, for the frequencies we have used to date, the upper medium reacts like a linear resistor, the current being constrained to flow in relatively thin upper formation by the zero conductivity of the lower formation.

The same condition is not true for the zero resistivity substratum. Currents are, in this case, free to flow unrestricted by geometrical boundaries. Hence,

even though the depth of the upper region is negligible, to the extent that at remote distances $\frac{E}{H}$ would be the same in both regions, pronounced effects in the region about the discontinuity can be observed.

The striking similarity between the corresponding curves of Figures 12 through 17, which differ only in the frequencies used, is probably only useful as a criterion that both frequencies are relatively low. The same information is obtainable in the case of a fault from the fact the values of $\frac{E}{H}$ are the same at remote distances from the fault in either media.

The phase angle variations, for the frequencies which we have measured and computed, are not sufficiently pronounced to warrant treatment. Further results from the computing centre will be more useful in the study of phase angles, since higher frequencies will be employed.

Experimental Results

The measured values of $\frac{E}{H}$ are plotted, together with the appropriate theoretical results, in Figures 12 through 17. It can be seen that the magnitudes of the experimental results are in reasonable agreement with curves corresponding to a zero resistivity substratum. This is also seemingly in accord with our previous conclusion, based on the frequency analysis, that our complicated

model of a layered earth was underlain by a very low resistivity substratum. It should be pointed out that an extrapolation of concepts based on a two-layered case to a more complicated case is hazardous. We have already seen that the conditions of the horizontal layering can have a very pronounced effect on the response due to a vertical discontinuity.

We have mentioned in Chapter VI that we measure the average field over the distance of the probe spacing. This is, of course, the same as the procedure in actual field measurements. Further, in our model we are unable to measure right up to the interface and hence are unable to measure in the most sensitive region for detecting variations in the field components. Despite these facts, the results do indicate a curvature in the correct direction.

In Figure 18, we have plotted the results of measurements in which a graphite dike of resistivity $8 \times 10^{-6}$ ohm-meters, and a resistive dike of resistivity larger than $10^{6}$ ohm-meters, and whose lateral dimensions are 10 cm square, have been immersed in a concentrated salt solution of depth 20 cm and resistivity $4 \times 10^{-2}$ ohm-meters. If we consider here scaling factors of $10^{4}$ then these correspond to dikes of depth 1 km buried to a depth of 1 km of overburden. In the case of the

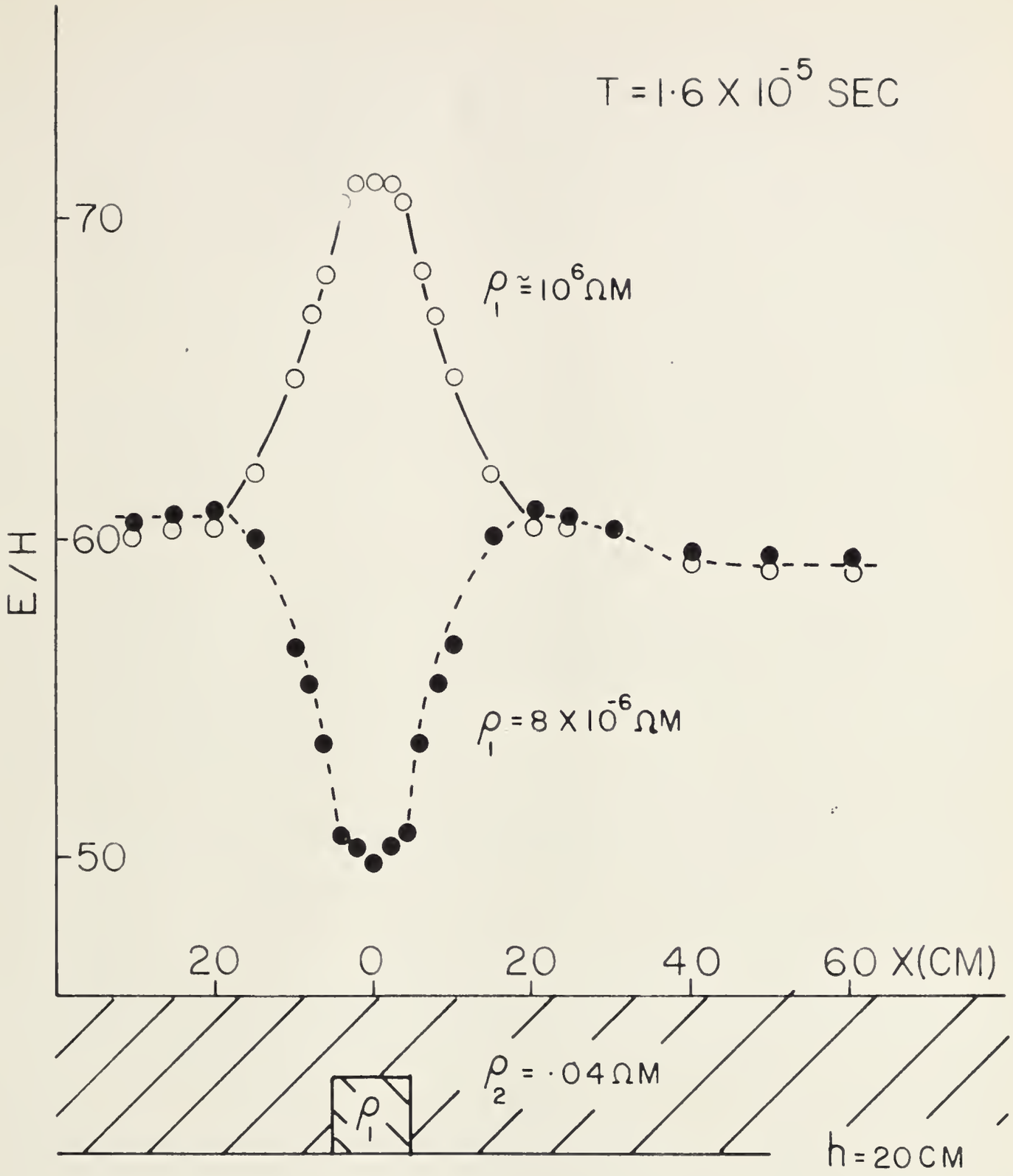


Fig. 18. The magneto-telluric ratio, on a linear scale, over high contrast dikes with deep overburden.

graphite dike this could correspond to massive sulphides surrounded by country rock, whereas the resistive dike could be considered as an igneous intrusion. We have plotted the magneto-telluric ratio on a linear scale because of low contrasts observed in the signals which have been attenuated by the 1 km of conducting material.

In Figure 19, are plotted the results obtained from traverses across these same two dikes immersed in a shallow layer of concentrated salt solution just deep enough to provide sufficient solution over the dikes to make electrical connections with the probes. This layer of depth 2 mm would correspond to 20 m of weathering using the same scaling factor as in the previous mentioned case.

Though the possibility of detecting either conducting or non-conducting bodies at appreciable depths is of considerable interest, the theoretical development for a geometry of this type has not yet been attempted. However, some understanding of the effect of overburden can be obtained from a study of these curves.

In Figure 20, is shown the variation in the magnetic field over a conducting dike. We have plotted this on a linear scale, in addition to the logarithmic, since the effect is quite small.

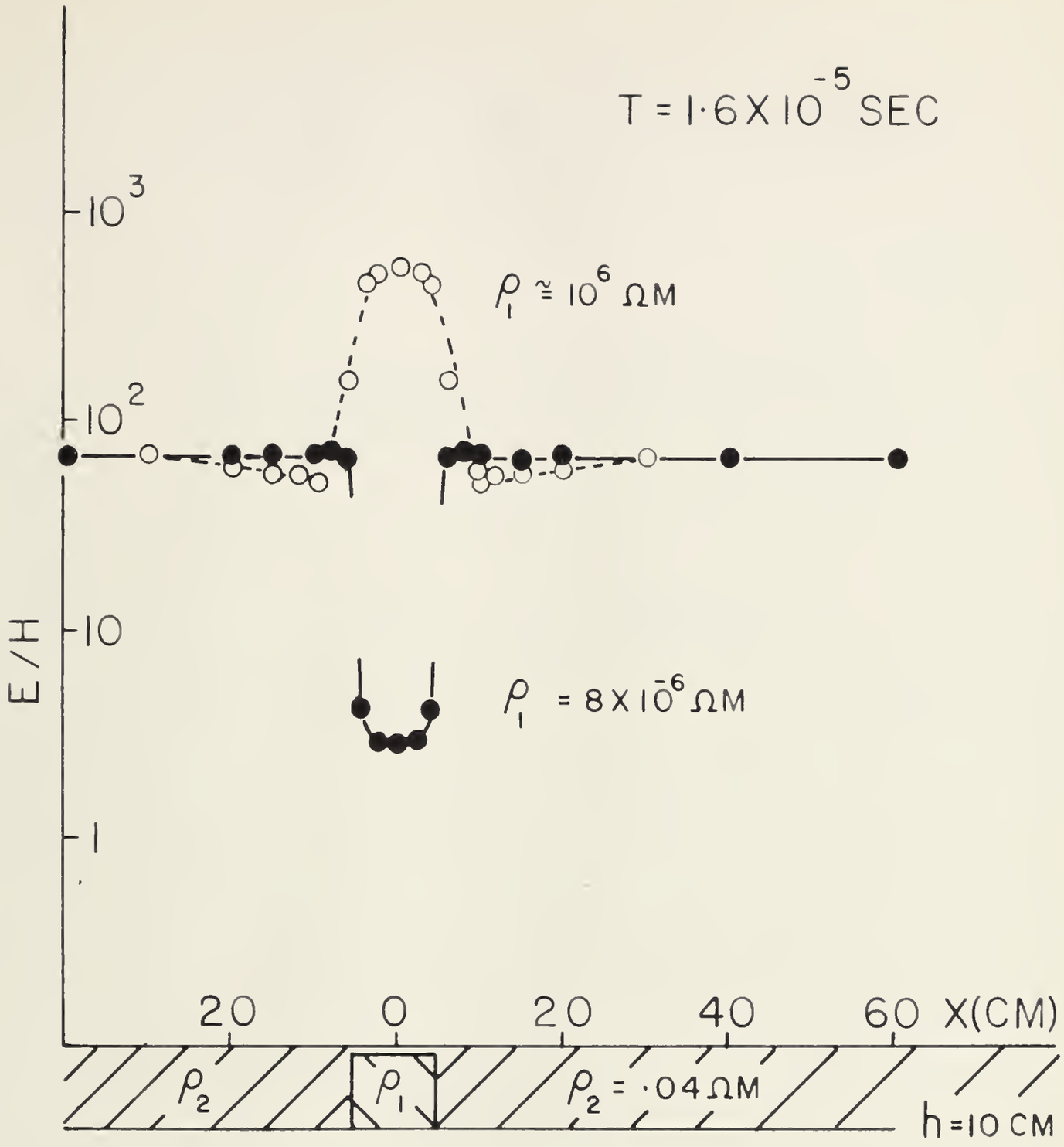


Fig. 19. The magneto-telluric ratio for high contrast dikes with shallow overburden.

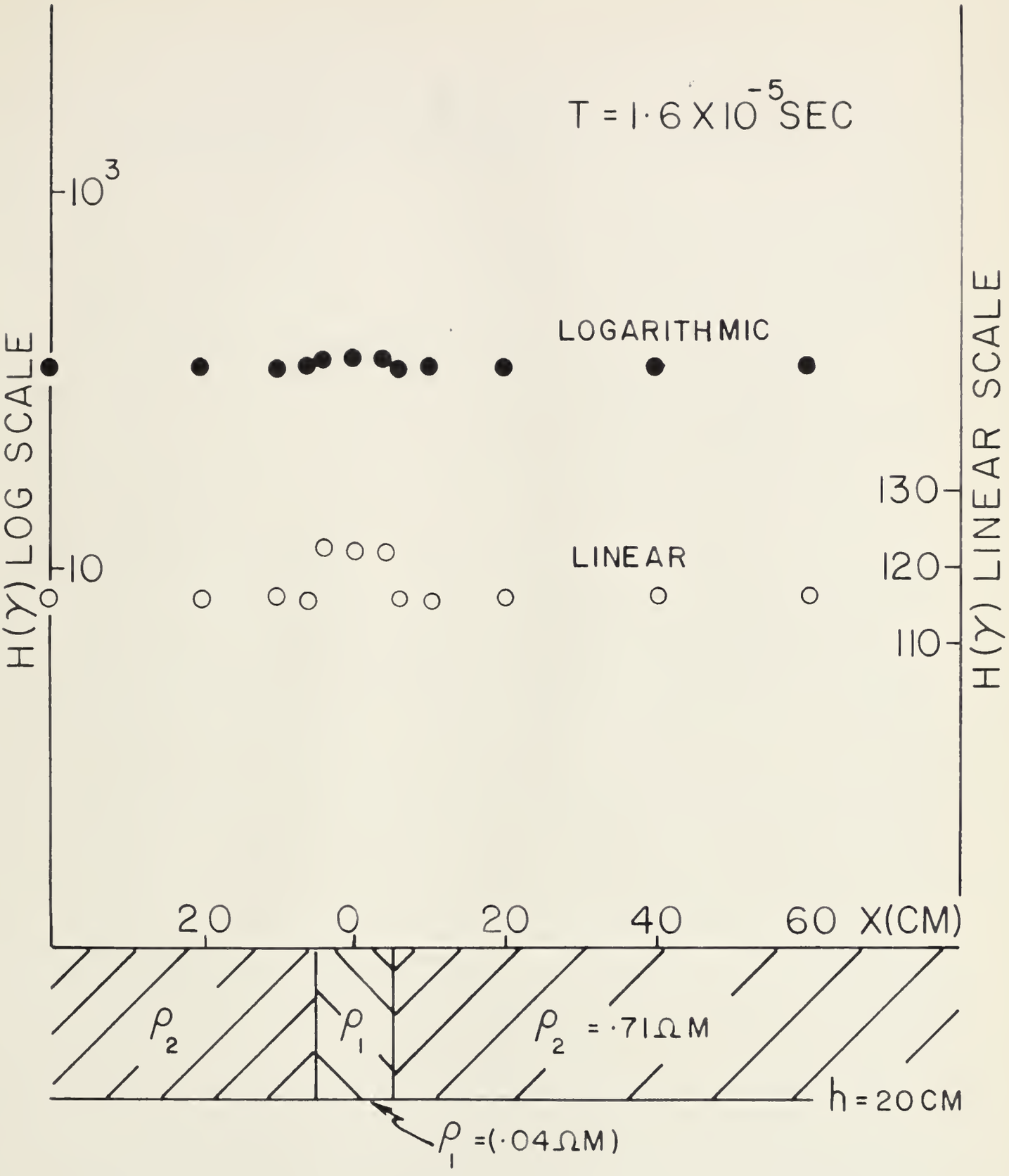


Fig. 20. The variation in the magnetic field over a discontinuity.

# CHAPTER VIII

## CONCLUSIONS AND SUGGESTIONS FOR FURTHER WORK

The value of a model study lies primarily in its role of advancing the understanding of phenomenon not directly susceptible to mathematical analysis. Before it is possible to proceed with confidence in applying model results to a real earth, quantitative verification of cases, for which analytic solutions do exist, is essential. While the experimental results of this work are in reasonable qualitative agreement with the existing theory, more exact correspondence would be desirable. To this end, a model incorporating a better approximation to either or both of the infinitely conducting or infinitely resistive substratum should be developed. The use of much higher frequencies would assist in this project, since the dimensions of the model could then be reduced, if the result of introducing shorted end plates is as effective as we assume. Further experimentation regarding this last point is required.

In the cases discussed in this work, where the magnetic field is polarized parallel to the structure, the validity of the assumption that the tangential component of the magnetic field is constant, is established

by the results shown in Figure 20. We feel confident, therefore, in proceeding to complete a catalogue of computed curves. By varying the different parameters, sets of curves can be obtained which will clearly illustrate the effect on the magneto-telluric field of various structures and resistivity contrasts.

The solution to the boundary value problems where the electric vector is parallel to the strike of the structure would be desirable. In the practical application in exploration known as "Afmag", the variation in the plane of polarization of the magnetic vector is measured near or at the surface of the earth.

The vertical component of the magnetic vector is believed to be due to the variation of the magnetic field across discontinuities when the polarization is in the direction as described above. In a more academic application, the long period variations in the vertical component of the magnetic field as measured at coastal observatories could perhaps be explained in terms of polarization at depth. In any event, the solution to this type of problem is inherently more difficult than the cases described in this work, since one can no longer assume the constancy of either field vector in crossing the trace of the discontinuity.

# APPENDIX I

This is a special case, the geometry of which is illustrated in Chapter III, Figure 4, where n = 1, $\rho_n = \rho$, and the single layer, in keeping with our original description, extends infinitely downward.

The propagation equation:

$$\frac{d^2 H_y}{dz^2} = 4\pi z \sigma \omega H_y$$

has a solution:

$$H_y = B e^{-\sqrt{j}\frac{z}{p}}$$

where p has been defined previously as:

$$p = \frac{1}{\sqrt{4\pi\sigma\omega}} .$$

There is no reflected wave since the medium is infinitely extended downward.

At the upper boundary, continuity of $H_y$ requires:

$$H_y(o) = H_o ,$$

where $H_o$ is the magnetic field in air, $H_y$ is the medium. Therefore:

$$H_y = H_c e^{-\sqrt{j}\frac{z}{p}} .$$

From Equation 4, Chapter II:

$$E_x = -\frac{\rho}{4\pi}\frac{\partial H_y}{\partial z}$$

provides that:

$$E_x = \frac{\rho\sqrt{j}}{4\pi\rho} H_o e^{-\sqrt{j}\frac{z}{\rho}}.$$

At the upper surface where z = 0:

$$E_x^{(o)} = \sqrt{j}\frac{\rho}{4\pi\rho} H_o .$$

Thus the measurement of:

$$\left(\frac{E_x}{H_y}\right)_o = \sqrt{j\frac{4\pi \cdot \omega}{(4\pi)^2 \cdot \sigma}} = \sqrt{j}\sqrt{\frac{x}{2T}}$$

relates the magneto-telluric ratio to the resistivity of the medium and the period T of electro-magnetic variation. We re-write this expression:

$$\left(\frac{E_x}{H_y}\right)_o = \sqrt{\frac{\rho}{2T}} e^{j\frac{\pi}{4}} .$$

Thus, for an infinite single layer, E leads H by 45° and the resistivity of the medium can be expressed:

$$\rho = 2T\left|\frac{E_x}{H_y}\right|^2 .$$

# APPENDIX II

## A TWO-LAYERED EARTH

This is a special case of the multi-layered earth illustrated in Figure 4, Chapter III, with n = 2. Formation 2 of resistivity $\rho_2$ extends infinitely downward.

The solution to the propagation equation:

$$\frac{d^2 H_y}{dz^2} = 4\pi j \sigma \omega H_y \qquad \text{(III-6)}$$

is:

$$H_i = A_i e^{\sqrt{j}\frac{z}{P_i}} + B_i e^{-\sqrt{j}\frac{z}{P_i}} \qquad \text{(III-7)}$$

$$P_i = \frac{1}{\sqrt{1 + \pi \rho_i \omega}} .$$

In Formation 1 the solution is:

$$H_y = A_1 e^{\sqrt{j}\frac{z}{P_1}} + B_1 e^{-\sqrt{j}\frac{z}{P_1}} ,$$

while in Formation 2 the solution is:

$$H_y = e^{-\sqrt{j}\frac{z}{P_2}} .$$

$E_x$ is obtained from $H_y$ by application of equation II-4 which in Formation 1 is:

$$E_x = \frac{-\rho_1}{4\pi}\frac{\sqrt{j}}{P_1}\left[A_1 e^{\sqrt{j}\frac{z}{P_1}} - B_1 e^{-\sqrt{j}\frac{z}{P_1}}\right] ,$$

while in Formation 2:

$$E_x = \frac{\omega \rho_2}{4\pi}\frac{\sqrt{j}}{P_2} e^{-\sqrt{j}\frac{z}{P_2}} .$$

The continuity of $H_y$ at $z = h$ results in:

$$A_1 e^{\sqrt{j}\,h_1} + B_1 e^{-\sqrt{j}\,h_2} = e^{-\sqrt{j}\,h_2} \qquad A\text{-}1$$

where

$$h_1 = \frac{h}{P_1} .$$

The continuity of $E_x$ at $z = h$ results in:

$$\frac{\rho_1}{P_1}\left[-A_1 e^{\sqrt{j}\,h_1} + B_1 e^{-\sqrt{j}\,h_1}\right] = \frac{\rho_2}{P_2} e^{-\sqrt{j}\,h_2} . \qquad A\text{-}2$$

Eliminating $e^{-\sqrt{j}\,h_2}$ between equation A-1 and A-2:

$$A_1 e^{\sqrt{j}\,h_1} + B_1 e^{-\sqrt{j}\,h_1} = \frac{\sqrt{\sigma_2}}{\sqrt{\sigma_1}}\left[-A_1 e^{\sqrt{j}\,h_1} + B_1 e^{-\sqrt{j}\,h_1}\right]$$

$$A_1 = B_1 e^{-2\sqrt{j}\,h_1}\left[\frac{\sqrt{\sigma_2} - \sqrt{\sigma_1}}{\sqrt{\sigma_2} + \sqrt{\sigma_1}}\right],$$

which when substituted back in equation A-1 gives:

$$B_1 = \frac{\sqrt{\sigma_2} + \sqrt{\sigma_1}}{2\sqrt{\sigma_1}} e^{\sqrt{j}\,(h_1 - h_2)}$$

and:

$$A_1 = \frac{\sqrt{\sigma_2} - \sqrt{\sigma_1}}{2\sqrt{\sigma_1}} e^{-\sqrt{j}\,(h_1 + h_2)} .$$

Thus, at the surface $z = 0$, we can write:

$$\frac{E_x}{H_y} = \frac{1}{\sqrt{2\sigma_1 T}} \frac{M}{N} e^{-i\left(\frac{\pi}{4} + \phi - \psi\right)}$$

where:

$$M \cos\phi = \left[\frac{1}{d_1}\cosh\frac{h}{d_1} + \frac{1}{d_2}\sinh\frac{h}{d_1}\right]\cos\frac{h}{d_1}$$

$$M \sin\phi = \left[\frac{1}{d_1}\sinh\frac{h}{d_1} + \frac{1}{d_2}\cosh\frac{h}{d_1}\right]\sin\frac{h}{d_1}$$

$$N \cosh\Psi = \left[\frac{1}{d_1}\sinh\frac{h}{d_1} + \frac{1}{d_2}\cosh\frac{h}{d_1}\right]\cos\frac{h}{d_1}$$

$$N \sin\Psi = \left[\frac{1}{d_1}\cosh\frac{h}{d_1} + \frac{1}{d_2}\sinh\frac{h}{d_1}\right]\sin\frac{h}{d_1} ,$$

and where:

$$d_i = \frac{1}{\sqrt{2\pi\sigma_i\omega}}$$

is the skin depth.

If one defines the apparent resistivity:

$$\rho_a = \rho_1\left(\frac{M}{N}\right)^2 ,$$

then it can easily be shown that:

$$\frac{\rho_a}{\rho_1} = 1 + \frac{4\cos\frac{2h}{d_1}}{m + \frac{1}{m} - 2\cos\frac{2h}{d_1}}$$

where:

$$m = \frac{\sqrt{\frac{\rho_2}{\rho_1} + 1}}{\sqrt{\frac{\rho_2}{\rho_1} - 1}}\, e^{\frac{2h}{d_1}} .$$

The analysis and interpretation is done in Chapter III.

# APPENDIX III

## SPECIAL CASE OF A TWO-LAYER EARTH WITH A FINITELY RESISTIVE UPPER FORMATION

We will treat in this appendix both the case of an infinitely resistive and an infinitely conductive substratum.

Case 1: Infinitely Resistive Substratum

The geometry is the same as in the previous example of the general two-layered earth illustrated in Figure 4, Chapter III, with n = 2.

The propagation equation in this case is:

$$\frac{d^2H}{dz^2} = \left[4\pi j\sigma\omega - \epsilon\omega^2\right] H$$

where the second term on the right is included to take into account propagation in Formation 2 where because $\sigma_2 = 0$, only the displacement current term is non-zero. In Formation 2 a solution has the form:

$$H_2 = B_2 e^{-j\frac{\omega}{c}z}$$

since there is at most a downgoing wave. It is obvious that there is no attenuation in Formation 2, which is what is to be expected in a non-dissipative medium.

In Formation 1, where the displacement current is negligible:

$$H_1 = A_1 e^{\sqrt{j}\frac{z}{p_1}} + B_1 e^{-\sqrt{j}\frac{z}{p_1}}$$

$$P_1 = \frac{1}{\sqrt{4\pi\sigma_1\omega}} ,$$

and at the boundary z = h,

$$A_1 e^{\sqrt{j}\frac{h}{\rho_1}} + B_1 e^{-\sqrt{j}\frac{h}{\rho_1}} = B_2 e^{-j\frac{\omega}{c}h} .$$

For any reasonable value of h, the thickness of the upper stratum, and for periods of interest for the magneto-telluric method, the exponent on the right hand side of the equation is approximately zero. Thus, writing in the usual way:

$$h_1 = \frac{h}{\rho_1} ,$$

we obtain:

$$A_1 e^{\sqrt{j}h_1} + B_1 e^{-\sqrt{j}h_1} = B_2 ,$$

and from the application of Maxwell's equation written in the form:

$$\nabla \times \vec{H} = 4\pi\sigma\vec{E} + \frac{\partial \vec{D}}{\partial t} ,$$

we have for our one dimensional geometry:

$$-\frac{dH_y}{dz} = \left[4\pi\sigma + j\varepsilon\omega\right] E_x .$$

For the upper formation where displacement current is negligible we obtain Equation II-4:

$$E_1 = \frac{-\rho_1}{4\pi}\frac{\partial H_1}{\partial z} ,$$

whereas in Formation 2 where $\sigma_2 = 0$

$$E = \frac{j}{\varepsilon\omega}\frac{\partial H_2}{\partial z}$$

At the boundary where z = h:

$$\frac{-\rho_1}{4\pi}\frac{\sqrt{j}}{P_1}\left[A_1 e^{\sqrt{j}h_1} - B_1 e^{-\sqrt{j}h_1}\right] = \frac{-B_2}{\sqrt{\varepsilon}} .$$

Eliminating $B_2$ between the two equations, we obtain:

$$\frac{\sqrt{\varepsilon}\,\rho_1}{+\pi}\frac{\sqrt{j}}{P_1}\left[A_1 e^{\sqrt{j}h_1} - B_1 e^{-\sqrt{j}h_1}\right] = A_1 e^{\sqrt{j}h_1} + B_1 e^{-\sqrt{j}h_1}$$

$$A_1 = B_1 \frac{e^{-2\sqrt{j}h_1}\left[\sqrt{j\varepsilon}\,\frac{\omega}{P_1} - 1\right]}{\left[\sqrt{j\varepsilon}\,\frac{\omega}{P_1} + 1\right]} .$$

In the approximation already introduced, where $\omega$ corresponds to periods of a few seconds and when skin depths are larger than a few meters, we can write:

$$A_1 = -B_1 e^{-2\sqrt{j}h} ,$$

in which case, by substituting back into the equation relating $B_2$ to $A_1$ and $B_1$, we find to the approximation we have made that:

$$B_2 = 0 .$$

At the upper surface, z = 0:

$$A_1 + B_1 = H_0 ,$$

therefore:

$$B_1 = \frac{H_0 e^{\sqrt{j}h_1}}{2\sinh(\sqrt{j}h_1)} , \qquad A-3$$

and:

$$A_1 = \frac{-H_0 e^{-\sqrt{j}h_1}}{2\sinh(\sqrt{j}h_1)} . \qquad A-4$$

The rather surprising result that the magnetic field vanishes at the surface of an infinitely resistive substratum may appear at first glance to be antithetical to the case of an infinitely conducting substratum, on the surface of which the electrical field must vanish. However, the situation is rather similar to the flow of energy in a wave guide in which there is a mismatched impedance element. Thus, that portion of an incoming wave which is not reflected at the first suface is trapped and dissipated within the conducting medium.

Writing the complete expression for the electric field:

$$E = \frac{+\rho}{4\pi} \frac{\sqrt{j}\, H_0}{P_1} \left[ \frac{e^{-\sqrt{j} h_1} e^{\sqrt{j} \frac{z}{P_1}} + e^{\sqrt{j} h_1 - \sqrt{j} \frac{z}{P_1}}}{2 \sinh(\sqrt{j} h_1)} \right],$$

we obtain for the magneto-telluric ratio at z = 0:

$$\left( \frac{E_x}{H_y} \right)_0 = \sqrt{\frac{j \rho_1}{2T}} \coth(\sqrt{j} h_1) \qquad A-5$$

Case 2: Infinitely Conducting Substratum

Proceeding as in the forementioned Case 1, we can write:

$$H = A e^{\sqrt{j} \frac{z}{P_1}} + B_1 e^{-\sqrt{j} \frac{z}{P_1}},$$

then writing the equation of continuity for Hy at z=0, and for $E_x$ at z=h:

$$A_1 + B_1 = H_o$$
$$A_1 e^{\sqrt{j}h_1} - B_1 e^{-\sqrt{j}h_1} = 0.$$

Eliminating $B_1$ between these two equations:

$$A_1 = \frac{H_o e^{-\sqrt{j}h_1}}{2\cosh(\sqrt{j}h_1)} \qquad A-6$$

$$B_1 = \frac{H_o e^{\sqrt{j}h_1}}{2\cosh(\sqrt{j}h_1)} \qquad A-7$$

we obtain:

$$E_x = \frac{-H_o \rho_1}{4\pi} \frac{\sqrt{j}}{P_1} \left[ e^{-\sqrt{j}h_1} e^{\sqrt{j}\frac{z}{P_1}} - e^{\sqrt{j}h_1} e^{-\sqrt{j}\frac{z}{P_1}} \right],$$

and finally:

$$\left(\frac{E_x}{H_y}\right)_o = \sqrt{j\frac{\rho_1}{2T}} \tanh(\sqrt{j}h_1). \qquad A-8$$

# APPENDIX IV

## A FAULT IN A TWO-LAYERED EARTH

We will discuss two special cases where the substratum resistivity is zero or infinite.

Case 1: An Infinitely Resistive Substratum

The geometry is illustrated in Figure 8, Chapter IV. Region 1 of resistivity $\rho_1$ and region 2 of resistivity $\rho_2$ are underlain by a uniform formation of infinite resistivity infinitely extended downward.

Following the procedure of d'Erceville and Kunetz (1959) outlined in Chapter IV, we write the solution in the upper formation:

$$H_i(x,y) = H_i(z) + P_i(x,z) .$$

For either region, where $P_i(x,z)$ is the term which is added to the solution for the simple layered system because of the disturbance, $P_i(x,z)$ is a function which vanishes for $|x| \to \infty$ and also for $z = 0$ and $z = h$. We therefore assume that we can write $P_i(x,z)$ as a product:

$$P_i(x,z) = f_i(x)\, g_i(z)$$

where further, $g_i(z)$ can be expanded as a Fourier series of argument $\frac{n\pi z}{h}$ . We proceed further and include the coefficient of $\sin \frac{n\pi z}{h}$ with $f_i(x)$ to write finally:

$$H_i(x,y) = H_i(z) + \sum f_{in}(x) \sin \frac{n\pi z}{h}$$

where each term on the left must satisfy the propagation equation:

$$\frac{\partial^2 H}{\partial x^2} + \frac{\partial^2 H}{\partial z^2} = +5\pi j\sigma\omega H.$$

As in Chapter IV this leads to the expression:

$$f_{in}(x) = a_{in} e^{-k_{in}\frac{x}{h}} + b_{in} e^{k_{in}\frac{x}{h}}$$

$$k_{in} = \sqrt{n^2\pi^2 + j h_i^2}, \quad h_i = h\sqrt{+\pi\sigma_i\omega}.$$

In the region of negative x only the term with a positive exponential can be valid, thus only the $b_{in}$ coefficients are non-zero. Similarly, only the $a_{in}$ coefficients are non-zero in the positive x region. At the boundary between regions 1 and 2 which is the y-z plane at x = 0, we require that both $H_y$ and $E_z$ are continuous:

$$P_1(0,z) + H_1(z) = P_2(0,z) + H_2(z).$$

Thus, if we expand $H_2 - H_1$ as a Fourier series of the same argument as in $P_1 - P_2$, we can equate at the boundary term by term both in $H_y$ and $E_z = \frac{\rho}{+5\pi} \frac{\partial H_y}{\partial x}$. The coefficient $A_n$ of $\sin \frac{n\pi z}{h}$ in the Fourier expansion of $H_2 - H_1$ is found by the standard method:

$$A_n = \frac{2}{h} \int_0^h (H_2 - H_1) \sin \frac{n\pi z}{h}\, dz.$$

The boundary conditions then yield:

$$a_{1n} - b_{2n} = A_n$$
$$k_{1n}\gamma_1 a_{1n} + k_{2n}\gamma_n b_{2n} = C \quad .$$

The expression for $H_2 - H_1$ for this case is found from equations A-3 and A-4 of Appendix III and the integration of $A_n$ is readily performed:

$$a_{1n} = 2\pi j H_o (h_1^2 - h_2^2) \frac{n}{k_{1n}^2 k_{2n}^2 \left[1 + \frac{h_2^2 k_{1n}}{h_1^2 k_{2n}}\right]}$$

with a similar expression for $b_{2n}$.

Writing H(x,z) explicitly:

$$H(x,z) = \frac{H_o}{2\sinh \sqrt{j} h_1} \left[-e^{-\sqrt{j} h_1} e^{\sqrt{j}\frac{z}{p_1}} + e^{\sqrt{j} h_1} e^{-\sqrt{j}\frac{z}{p_1}}\right]$$

$$+ 2\pi j H_o (h_1^2 - h_2^2) \sum \frac{n e^{-k_{1n}\frac{x}{h}} \sin \frac{n\pi z}{h}}{k_{1n}^2 k_{2n}^2 \left[1 + \frac{h_2^2 k_{1n}}{h_1^2 k_{2n}}\right]} \quad ,$$

we can find $E_x$ and finally the magneto-telluric ratio at z = 0 in both regions. In region 1:

$$\frac{E_1}{H_o} = \sqrt{j}\,\frac{\omega h}{h_1} \coth(\sqrt{j} h_1) - 2\pi^2 j \omega h \frac{(h_1^2 - h_2^2)}{h_1^2} U_1$$

$$U_1 = \sum_{n=1}^{\infty} \frac{n^2 e^{-k_{1n}\left|\frac{x}{h}\right|}}{k_{1n}^2 k_{2n}^2 \left[1 + \frac{h_2^2 k_{1n}}{h_1^2 k_{2n}}\right]} \quad .$$

The magneto-telluric ratio for region 2 is found

from the preceding expression by a simple interchange of subscripts.

Case 2: An Infinitely Conducting Substratum

In this case all the results of the previous section hold, except that exactly as in Chapter IV for this substratum we expand g(z) as a sin series of argument $\frac{n\pi z}{2h}$ since in:

$$P_i(x,z) = f_i(x)\, g_i(z)$$

we must have a disturbance function which vanishes for $|x| \to \infty$ and z = 0, but which has a finite value at z = h. Therefore, when we also expand $H_2 - H_1$, as a Fourier sin series also in $\frac{n\pi z}{2h}$ we must define:

$$H_2 - H_1 = F(z) \qquad 0 \le z \le h$$

$$H_2 - H_1 = F(2h-z) \qquad h \le z \le 2h$$

where $H_2$ and $H_1$ are the appropriate solutions for the simple double-layer system of Case 2, Appendix III.

When this procedure is carried out, we obtain the magneto-telluric ratios:

$$\frac{E}{H_o} = \frac{\omega h}{h_1}\sqrt{j}\tanh\left(\sqrt{j}\,h_1\right) - 8\pi^2 j\,\omega h\left[\frac{h_1^2 - h_2^2}{h_1^2}\right] U_1$$

$$U_1 = \sum_{n=0}^{\infty} \frac{(2n+1)^2\, e^{-k_{1n}\left|\frac{x}{2h}\right|}}{k_{1n}^2 k_{2n}^2\left[1 + \frac{h_2^2 k_1}{h_{1n}^2 k_{2n}}\right]} \,,$$

with:

$$k_m = \sqrt{(2n+1)^2 \pi^2 + 4 j h_1^2} \quad .$$

$\frac{E_2}{H_o}$ is again obtained from $\frac{E_1}{H_o}$ by a simple interchange of subscripts.

# BIBLIOGRAPHY

Barlow, W. H., (1849): "On the spontaneous electric currents observed in the wires of the electric telegraph." Phil. Trans. 139, 61 - 72.

Bartels, J., (1954): Nach. Akad. Wiss. Göttingen (Phys. Math. Kl.) Abt. IIa, 95 100.

Cagniard, L., (1953): "Basic Theory of the Magneto-telluric Method". Geophysics 8, 605 - 635.

Cagniard, L., (1954): Correspondence between J. R. Wait and L. Cagniard, Geophysics 18, 286 - 289.

Cagniard, L., (1956): "Ellectricite tellurique" Handbuch der Geophysik, 17, 407 - 468, Verlag Julius Spenger.

Cantwell, T., (1960): "Detection and Analysis of Low Frequency Magneto-telluric Signals." Ph.D. Thesis, M.I.T.

Chapman, S., (1919): "The solar and lunar diurnal variations of terrestrial magnetism." Phil. Trans. Roy. Soc. A218, 1 - 118.

d'Erceville, I., and Kunetz, G., (1959): "Some observations regarding natural electromagnetic fields in applied geophysics." Paper at S.E.G. meeting in Los Angeles.

Gish, O. H., (1936): "Electrical messages from the earth; their reception and interpretation." J. Wash. Acad. Sci. 26, 267 - 289.

Kato, Y.,and Kikuchi, T., (1950): "On the phase difference of earth currents induced by the changes of the earth's magnetic field." Tohoku Univ. Sc. Rep. 5th ser. Geophysics 2, 2, 138 - 145.

Kunetz, G., (1953): "Correlation et recurrence des variations des courants telluriques et du champ magnetique". Actes du Congres de Lux. 72 eme Ses. de l'Association pour l'Advancement des Sciences.

Kunetz, G., (1954): "Enregistrement des Courants telluriques a l'occasion de l'eclipse de soleil du 25 Febrier, 1952". Anal. Geoph. 10, 262.

Lipskaia, N.V., (1953): "Some correlations between harmonics of periodic variations of terrestrial electromagnetic fields." Akad. Nauk. S.S.S.R. Izv. Serv.-Geofix. I, 41 - 47.

McNish, A. G., (1939): "On causes of the earth's magnetism and its changes." Terrestrial Magnetism and Electricity, ed Fleming, McGraw-Hill Book Co., Inc., New York.

Neves, A. S., (1957): "The magneto-telluric method in two dimensional structures." Ph. D. Thesis, M.I.T.

Rikitake, T., (1951): "Changes in earth currents and their relation to the electrical state of the earth's crust." Bull. Earthq. Res. Inst. Tokyo, 29, 270 - 275.

Rikitake, T., Yokohama, I., and Hishiyama, Y., (1952): Bull. Earthq. Res. Inst. Tokyo, 30, 207. (1953): 31, 19, 89, 101, 119.

Rikitake, T., and Yokohama, I., (1955): Bull. Earthq. Res. Inst. Tokyo, 33, 297 - 331.

Rooney, W. J. (1939): "Earth Currents"; Terrestrial Magnetism and Electricity, ed Fleming, McGraw-Hill Book Co., Inc., New York.

Schelkunoff, S. A., (1938): "The impedance concept and its application to problems of reflection, refraction, shielding, and power absorption." Bell System Tech. Jour. 17, 17.

Schlumberger, M., and Kunetz, G., (1946): "Variations rapides simultanees du champ tellurique en France et a Madagascar". C.R. Acad. Sci. Paris 223, 551 - 553.

Schuster, A., (1889): "The diurnal variation of terrestrial magnetism." Phil. Trans. Roy. Soc. London, A 180, 467 - 512.

Stratton, J. A., (1941): "Electromagnetic Theory", McGraw-Hill Book Co., Inc., New York.

Tikhonov, A. N., (1950): Dokl. Akad. Nauk. S.S.S.R. 73, 295.

Wait, J. R.,(1954): "On the relations between telluric currents and the earth's magnetic field." Geophysics 19, 281 - 289.